

Spring 5-25-2019

# The Real-Time Application of Control Theory to Pharmacokinetics

George W. Carpenter III  
*Louisiana Tech University*

Follow this and additional works at: <https://digitalcommons.latech.edu/theses>

---

## Recommended Citation

Carpenter, George W. III, "" (2019). *Thesis*. 20.  
<https://digitalcommons.latech.edu/theses/20>

This Thesis is brought to you for free and open access by the Graduate School at Louisiana Tech Digital Commons. It has been accepted for inclusion in Master's Theses by an authorized administrator of Louisiana Tech Digital Commons. For more information, please contact [digitalcommons@latech.edu](mailto:digitalcommons@latech.edu).

**THE REAL-TIME APPLICATION OF CONTROL THEORY  
TO PHARMACOKINETICS**

by

George W. "Trey" Carpenter III, B.S. Electrical Engineering

A Thesis Presented in Partial Fulfillment  
of the Requirements of the Degree  
Master of Science

COLLEGE OF COLLEGE OF ENGINEERING & SCIENCE  
LOUISIANA TECH UNIVERSITY

May 2019

LOUISIANA TECH UNIVERSITY  
THE GRADUATE SCHOOL

**JUNE 28, 2018**

Date

We hereby recommend that the thesis prepared under our supervision by  
**George W. "Trey" Carpenter III, B.S. Electrical Engineering**  
entitled **The Real-Time Application of Control Theory to Pharmacokinetics**

be accepted in partial fulfillment of the requirements for the Degree of  
**Master of Science in Mathematics**

\_\_\_\_\_  
Supervisor of Thesis Research

\_\_\_\_\_  
Head of Department

\_\_\_\_\_  
Department

Recommendation concurred in:

\_\_\_\_\_  
\_\_\_\_\_  
\_\_\_\_\_  
\_\_\_\_\_

Advisory Committee

**Approved:**

\_\_\_\_\_  
Director of Graduate Studies

\_\_\_\_\_  
Dean of the College

**Approved:**

\_\_\_\_\_  
Dean of the Graduate School

## **ABSTRACT**

An optically-based injection control system has been developed as a proof-of-concept that such is of use for an intravenous drug delivery application. Current clinical drug delivery for oncology typically provides for intravenous administration without providing awareness of achieved plasma concentration, yet interpatient variability produces consequences ranging from toxicity to ineffectual treatments. We report a closed loop injection system integrating a pulse-photoplethysmograph to measure the concentration of indocyanine green (ICG) in the circulating blood of a one-compartment murine model. A proportional-derivative (PD) controller manages the injection rate in real-time. The target function for the controller is the population estimate of the pharmacokinetic model developed using Bayesian statistics describing the injection phase of a calibration set of 22 injections in mice. The controlled set of 8 injections showed a reduction in variance from the target injection phase concentration profile of 74.8%.

## APPROVAL FOR SCHOLARLY DISSEMINATION

The author grants to the Prescott Memorial Library of Louisiana Tech University the right to reproduce, by appropriate methods, upon request, any or all portions of this Thesis. It is understood that "proper request" consists of the agreement, on the part of the requesting party, that said reproduction is for his personal use and that subsequent reproduction will not occur without written approval of the author of this Thesis. Further, any portions of the Thesis used in books, papers, and other works must be appropriately referenced to this Thesis.

Finally, the author of this Thesis reserves the right to publish freely, in the literature, at any time, any or all portions of this Thesis.

Author George W. "Grey" Carpenter

Date 2/25/19

## **DEDICATION**

This thesis is dedicated first to my family for their unwavering support in its completion, second to my adviser team for the amazing guidance and invaluable input they provided, and lastly to all others who gave their time, hard-work, and determination in its creation.

## TABLE OF CONTENTS

ABSTRACT.....	iii
APPROVAL FOR SCHOLARLY DISSEMINATION .....	iv
DEDICATION .....	v
LIST OF FIGURES .....	viii
LIST OF TABLES .....	xi
ACKNOWLEDGMENTS .....	xii
CHAPTER 1 LITERATURE REVIEW .....	1
1.1    Current Medical Treatments .....	1
1.2    Control Theory in the Medical Field .....	2
1.3    Previous Work .....	3
1.4    Project Goals.....	4
1.5    Statistical and Computation Methods .....	5
CHAPTER 2 MATERIALS AND METHODS .....	11
2.1    Experimental Setup.....	11
2.2    Injections of ICG in Mice .....	11
2.3    The Photoplethysmograph .....	12
2.4    Bayesian Analysis.....	13
CHAPTER 3 PHARMACOKINETIC MODEL IDENTIFICATION .....	15
3.1    The Population Pharmacokinetic Model.....	15
CHAPTER 4 CONTROL SYSTEM AND TUNING.....	18
4.1    Selected Control System.....	18

4.2	Control System Tuning.....	19
4.3	Control Software.....	21
4.4	Analysis of Controller.....	22
CHAPTER 5 RESULTS .....		23
5.1	Data Inclusion Criteria.....	23
5.2	Population Pharmacokinetic Model.....	24
5.3	Analysis of Controlled Injections .....	25
CHAPTER 6 DISCUSSION.....		30
6.1	Overview.....	30
6.2	Controller Advantages .....	30
6.3	Pharmacokinetic Observations .....	31
6.4	Controller Error Response .....	31
6.5	General Outcome .....	32
6.6	Project Drawbacks .....	32
CHAPTER 7 CONCLUSIONS .....		34
7.1	Future Work.....	34
APPENDIX A CALIBRATION DATA MODELS AND VALIDATION DATA.....		36
APPENDIX B CODE FOR SOFTWARE & STATISICAL ANALYSIS .....		63
BIBLIOGRAPHY.....		69

## LIST OF FIGURES

<b>Figure 3-1:</b> Flow chart describing distribution of mice within experimentation parameters. ....	17
<b>Figure 5-1:</b> (Left) Example photoplethysmograph output of absorbance vs. time from mouse injection for an uncontrolled injection. (Right) Corresponding heartrate data from each wavelength (660 nm, 805 nm, and 940 nm) over a 1 min. interval. ....	24
<b>Figure 5-2:</b> (Left) model comparison error of 22 injections from the controlled group represented as a standard box plot about the average (solid line) approximately 0. (Right) model comparison error of 8 injections from the controlled group as a standard box plot about the average (dashed line) approximately -0.3, calibration average (solid line) provided for comparison .....	26
<b>Figure 5-3:</b> (Left) Example absorbance with time with injection control. (Right) Corresponding PD error and calculated injection-phase rate change. The dashed line is an asymptote of error (averaged) and solid line on left is the population pharmacokinetic model. ....	27
<b>Figure 5-4:</b> Injections from Controlled Data Set (dots) with target model (solid line) and 95% credible interval (dashed line), absorbance vs. time. Figures (a) – (c) have a final absorbance target of 2.25, figures (d) – (f) have a final absorbance target of 3.00, and figures (h) – (g) have a final absorbance target of 3.75. ....	29
<b>Figure A-1:</b> (Top) Injection profile M1I1 (dots) with model (red line) and (bottom) heart rate data averaged over 5 (red line), 10 (green line), and 15 (blue line) seconds. ...	37
<b>Figure A-2:</b> (Top) Injection profile M1I2 (dots) with model (red line) and (bottom) heart rate data averaged over 5 (red line), 10 (green line), and 15 (blue line) seconds. ...	38
<b>Figure A-3:</b> (Top) Injection profile M2I1 (dots) with model (red line) and (bottom) heart rate data averaged over 5 (red line), 10 (green line), and 15 (blue line) seconds. ...	39
<b>Figure A-4:</b> (Top) Injection profile M2I2 (dots) with model (red line) and (bottom) heart rate data averaged over 5 (red line), 10 (green line), and 15 (blue line) seconds. ...	40
<b>Figure A-5:</b> (Top) Injection profile M2I3 (dots) with model (red line) and (bottom) heart rate data averaged over 5 (red line), 10 (green line), and 15 (blue line) seconds. ...	41

**Figure A-6:** (Top) Injection profile M3I1 (dots) with model (red line) and (bottom) heart rate data averaged over 5 (red line), 10 (green line), and 15 (blue line) seconds. ... 42

**Figure A-7:** (Top) Injection profile M3I2 (dots) with model (red line) and (bottom) heart rate data averaged over 5 (red line), 10 (green line), and 15 (blue line) seconds. ... 43

**Figure A-8:** (Top) Injection profile M3I3 (dots) with model (red line) and (bottom) heart rate data averaged over 5 (red line), 10 (green line), and 15 (blue line) seconds. ... 44

**Figure A-9:** (Top) Injection profile M3I4 (dots) with model (red line) and (bottom) heart rate data averaged over 5 (red line), 10 (green line), and 15 (blue line) seconds. ... 45

**Figure A-10:** (Top) Injection profile M4I1 (dots) with model (red line) and (bottom) heart rate data averaged over 5 (red line), 10 (green line), and 15 (blue line) seconds. ... 46

**Figure A-11:** (Top) Injection profile M5I1 (dots) with model (red line) and (bottom) heart rate data averaged over 5 (red line), 10 (green line), and 15 (blue line) seconds. ... 47

**Figure A-12:** (Top) Injection profile M5I2 (dots) with model (red line) and (bottom) heart rate data averaged over 5 (red line), 10 (green line), and 15 (blue line) seconds. ... 48

**Figure A-13:** (Top) Injection profile M5I3 (dots) with model (red line) and (bottom) heart rate data averaged over 5 (red line), 10 (green line), and 15 (blue line) seconds. ... 49

**Figure A-14:** (Top) Injection profile M5I4 (dots) with model (red line) and (bottom) heart rate data averaged over 5 (red line), 10 (green line), and 15 (blue line) seconds. ... 50

**Figure A-15:** (Top) Injection profile M6I1 (dots) with model (red line) and (bottom) heart rate data averaged over 5 (red line), 10 (green line), and 15 (blue line) seconds. ... 51

**Figure A-16:** (Top) Injection profile M6I2 (dots) with model (red line) and (bottom) heart rate data averaged over 5 (red line), 10 (green line), and 15 (blue line) seconds. ... 52

**Figure A-17:** (Top) Injection profile M6I3 (dots) with model (red line) and (bottom) heart rate data averaged over 5 (red line), 10 (green line), and 15 (blue line) seconds. ... 53

**Figure A-18:** (Top) Injection profile M7I1 (dots) with model (red line) and (bottom) heart rate data averaged over 5 (red line), 10 (green line), and 15 (blue line) seconds. ... 54

**Figure A-19:** (Top) Injection profile M8I1 (dots) with model (red line) and (bottom) heart rate data averaged over 5 (red line), 10 (green line), and 15 (blue line) seconds. ... 55

**Figure A-20:** (Top) Injection profile M8I2 (dots) with model (red line) and (bottom) heart rate data averaged over 5 (red line), 10 (green line), and 15 (blue line) seconds. ... 56

**Figure A-21:** (Top) Injection profile M8I3 (dots) with model (red line) and (bottom) heart rate data averaged over 5 (red line), 10 (green line), and 15 (blue line) seconds. ... 57

**Figure A-22:** (Top) Injection profile M8I4 (dots) with model (red line) and (bottom) heart rate data averaged over 5 (red line), 10 (green line), and 15 (blue line) seconds. ... 58

**Figure A-23:** Validation Injection profile M1I1, (dots) with population model (red line). ..... 59

**Figure A-24:** Validation Injection profile M1I2 (dots) with population model (red line). ..... 59

**Figure A-25:** Validation Injection profile M1I3 (dots) with population model (red line). ..... 60

**Figure A-26:** Validation Injection profile M1I4 (dots) with population model (red line). ..... 60

**Figure A-27:** Validation Injection profile M2I1 (dots) with population model (red line). ..... 61

**Figure A-28:** Validation Injection profile M2I2 (dots) with population model (red line). ..... 61

**Figure A-29:** Validation Injection profile M2I3 (dots) with population model (red line). ..... 62

**Figure A-30:** Validation Injection profile M2I4 (dots) with population model (red line). ..... 62

**Figure B-31:** Process flow diagram for Python Control Software..... 64

## LIST OF TABLES

<b>Table 5-1:</b> Population pharmacokinetic model parameters based on calibration trials (n=22).....	25
<b>Table 5-2:</b> Comparison between expected dose (Exp) and achieved dose (Inj) necessary to achieve a target absorbance in validation experiments. ....	28

## **ACKNOWLEDGMENTS**

I would like to acknowledge Dr. D. P. O’Neal for the use of his lab and the use of the nanotracker (PPG) technology, previous developed by his lab and students. I would like to acknowledge Dr. Eric Sherer for his keen eye and expertise in the field of pharmacokinetics. I would like to acknowledge Dr. Katie Evans for the unwavering guidance during the tenure of this project as my major advisor and for her invaluable input involved in the solving of the equations which it entails, as well as her input in the field of controls. I would like to acknowledge Holly Meyers for her ever vigilant assistance on this project in both support and in handling the mice, without her this project would have taken considerably longer. And lastly, but certainly not least, I would like to acknowledge Dr. Teresa Murray for the donation of the mice used in the creation and implementation of this project, without which this project would have been only in theory.

# **CHAPTER 1**

## **LITERATURE REVIEW**

### **1.1 Current Medical Treatments**

The administration of medication has been simplified to the five rights: right medication, right dose, right patient, right time, and right route as a first approximation of the appropriate use of drugs [1]. This mantra neglects the variance observed between patients and between doses on the same patient in both pharmacokinetics (i.e., drug concentration dynamics) and pharmacodynamics (i.e., effects of these concentrations). Although the vast majority of drugs that receive Food and Drug Administration (FDA) approval have a broad therapeutic window – the range of doses at which a drug is effective without unacceptable adverse events – many drugs are available with a narrow therapeutic window because the potential benefits outweigh the side effects. For example, many chemotherapeutic agents fall into this category [1].

For drugs with a narrow therapeutic window, the concentration can be monitored over time to be within that window based on an individual patient's response. These adjustments can be made over a longer period of time based on the pharmacodynamics (e.g., titrating the dose of warfarin or adjusting the chemotherapy dose based on neutrophil counts) or over shorter time scales by adjusting the dose based on the pharmacokinetics. In theory, adjustments based on pharmacokinetics can be performed

during clinical drug administration and the area of therapeutic drug monitoring has arisen to regulate the effects of narrow therapeutic index drugs by controlling the pharmacokinetics. However, one of the limitations of therapeutic drug monitoring is the logistics of measuring blood concentrations at regular intervals and providing timely feedback during a single dose. Clinical therapeutic drug monitoring is generally restricted to measuring the pharmacokinetics during a dose and then adjusting subsequent doses based on the measured, patient-specific pharmacokinetics [1]. Herein, we demonstrate an enhancement of therapeutic drug monitoring in which the drug concentration is measured in real-time using optical sensing which allows for controlling the concentration of a drug during a dose rather than waiting for the next dose.

An example of the issues mentioned above may be seen in the in the field of anesthetics. It is a well-documented issue that monitoring of the drug delivery and the various states of the patient are crucial to maintaining the proper therapeutic and patient response. Such issues have seen marked improvement through the application of control systems monitoring vitals such as heartrate and mean arterial blood pressure [2].

## **1.2 Control Theory in the Medical Field**

Control theory has recently begun to branch into the field of medicine through a plethora of new and impactful avenues. These are as broad as the application of robotic arms to surgical procedures, to the specific implementation of control theory as a manner to interface directly with human neurons [3]. Other reports have demonstrated the use of proportional-integral-derivative (PID) control [4, 5, 6, 7] with pharmacometrics or fuzzy logic theories [3] to manage the dosing of anesthesia or drugs in a clinical setting. It is this burgeoning development of potential within the field of control theory that this

project was intended to adapt to the field of pharmacokinetics. Control in this setting can refer to the ability to manage a physiological variable within a desirable range, such as heart rate or blood pressure or brain activity, as well as the restriction of a drug concentration in vivo within a therapeutic dosing window. A significant limiting factor towards implementing control was the availability, or the lack thereof, of an associated sensing system to track an instantaneously relevant physiological state.

### **1.3 Previous Work**

Previously this lab implemented a three-wavelength photoplethysmograph (PPG) which measures the absorbance (which is related to concentration through Beer's Law) of optically active compounds in circulation, which was employed in this report to provide for real-time feedback. This device was used to measure the concentration of a circulating dose of optically absorptive gold nanoshells (a ~100 nm diameter particle) used in medical applications such as cancer therapy [8] as well as two drugs: amphotericin B [9] and quinine [10]. The probe is physically similar to a pulse oximeter and uses a finger or murine tail/leg clip. The precision of the instrument to provide a point estimate of concentration of these nanoparticles, relative to the measurement via off-line external blood draws, was reported to be  $\pm 20\%$  in the relevant concentration ranges. There has also been considerable prior work in this lab pertaining to the application of Bayesian modeling to the fields of biomedical technology and medical therapy, as can be seen in Magaña, et. al [11].

It is also important to provide cases of previous work founded in the field of medical controls, as this field only became viable in the last century. Throughout the latter half of the 20<sup>th</sup> century and over the last 20 years, there has been a wide range of

work in the field of medically applied controls. This ranges from applying controls to the medical field for monitoring the blood glucose level of a patient in a diabetic coma [12] work from the mid 70's, to the application in cases such as analyzing different potential methods of delivering chemotherapy drugs [13], a case similar in idea to this project. In the latter project, it is used as an adaptive, closed-loop method to model and control patient blood glucose level via state space, with the noted requirement of relevant patient data being readily available and viable to collect, it is then a simple matter of minimizing a set evaluation function which represents the effect treatment of the patient [12]. In the analysis of potential chemotherapy, varying robust optimal controllers were modeled and analyzed for their efficacy in treating cancer via chemotherapy, several key notes from this project included noting that the less model data that could be obtained, the more drug would have to be administered, and recommending the use of  $H_\infty$  when an initial dose of drug will not have a negative side effect, as doing so will reduce the overall amount of drug needed in treatment [13]. Though these are generally theoretical in their treatment of the field, they still provide a good background for the work done in this project, as a window into what could be expected.

#### **1.4 Project Goals**

The primary objective of this thesis is to demonstrate a system that controls the shape of the concentration versus time curve of a drug during injection by varying the injection rate of the drug in response to real-time concentration measurements to affect a reduction on the interpatient variability of blood concentration. Here interpatient variability at blood concentration is defined as the amount an individual's blood concentration varied from the population pharmacokinetic model. This system controls

the infusion rate thus providing the recommended drug concentration. A patient receiving the recommended concentration is more likely to result in an effective treatment (by ensuring under-exposure does not occur) with fewer adverse side effects (by ensuring over-exposure does not occur). To achieve this objective, a population model for the selected drug, ICG, was calibrated on a BALB/c mouse model; then developed a proportional-differential feedback control system (PDCS) that uses real-time absorbance measurements from the PPG as feedback; and then quantified the total delivered dose and verified we could track a target concentration versus time curve through the implementation of the control system on BALB/c mice to ensure it was effective in fulfilling its purpose of reducing variance within the therapeutic window.

## **1.5 Statistical and Computation Methods**

It is first necessary in this section to mention the method by which the statistical analysis was carried out during this work. For analysis of the data obtained during this project Markov Chain Monte-Carlo (MCMC) modeling was utilized via the WinBUGS analysis package, run using the R programming language. And it is also prudent before discussing MCMC to give a brief introduction into Bayes' theorem, as it is an integral foundation of the MCMC process.

The focus of this project in the field of pharmacokinetics was based on the principles of Bayesian modeling, i.e. the drug concentration within a patient body was the given system data utilized in conjunction with a model parameter vector treated as random variables by Bayes' theorem. Bayes' theorem as it applies to a system involving a model with a parameter vector may be seen below, **(1.1)**.

$$p(\bar{\theta}|y) = \frac{p(y|\bar{\theta}) p(\bar{\theta})}{p(y)} \quad (1-1)$$

In (1.1)  $p$  represents a probability density; this of course means  $p(\bar{\theta})$  is the prior distribution of the parameter vector set  $\bar{\theta}$ , that is; the distribution of the parameter set without consideration of the model prediction  $y$ , which are the values utilized to satisfy the model at the given inputs to achieve the value  $y$ . Thus  $p(y|\bar{\theta})$  is used to show how the data are predicted based on the parameter values and  $p(\bar{\theta}|y)$  is the posterior distribution for  $\bar{\theta}$ .

Here, as an aside, it should be noted that the parameter set  $\bar{\theta}$  represents the variables  $CL$ ,  $V$ , and  $\varphi_0$  of the functional form of the model seen in section 3.1 in (3.2), and the “inputs” to this model as referred to in this explanation are the time values  $t$  which correspond to the given  $y$ .

In general to use Bayes’ theorem in a practical way it was necessary to employ an algorithmic process, as mentioned above, for the purposes of this project, MCMC was selected as this implementation. In the application of MCMC it does not matter what happens with  $y$  in  $p(y|\bar{\theta})$ , as the model prediction  $y$  is the output from the system that is being modeled by this process. This means that for the purposes of modeling this system using MCMC, the term  $p(y|\bar{\theta})$  is obtuse, as it expects the probability of an unchanging data point (no longer model prediction as with Bayes’ theorem),  $y$ , to change as the

— — —  
 values of  $\bar{\theta}$  change. Therefore, we may replace  $p(y|\bar{\theta})$  with a mean-likelihood estimator (MLE) for  $\theta$ ,  $L(\theta; y)$ ; which will tell us the likelihood that our  $\theta$  fits the model, in its’ attempt to generate the known data point  $y$ . Thus, to restate (1.1) in this way as it applies to MCMC, we end up with (1.2) [14].

$$p(\bar{\theta}|y) \propto L(\bar{\theta}; y)p(\bar{\theta}) \quad (1-2)$$

In (1.2)  $p(\bar{\theta}|y)$  is proportional to the MLE,  $L(\bar{\theta}; y)$ , by the probability of  $\bar{\theta}$ ,  $p(\bar{\theta})$ .

It is this likelihood estimator that is key in determining the value of the posterior  $p(\bar{\theta}|y)$  and therefore the values of the parameter set. Often times to simplify the calculations, a conjugate will be used in place of the likelihood estimator  $L(\bar{\theta}; y)$ . A conjugate is a family of functions which describe the distribution of the prior and posterior, an example of this would be saying both distributions were Normal, thus using a Normal distribution to satisfy the given prior and posterior in (1.2) simplifies the calculation greatly [14].

It was clear then, from these observations, and prior work in the field of pharmacokinetics, that Bayesian statistics was the appropriate method for developing a population model for this project as it allowed for rapid prediction model for each test mouse [11]. This implementation is what allowed the project to perform under the constraints applied, such as number of mice available for data collection, and set equation creation. In other words, under the limitations of complexity, a one compartment pharmacokinetic model, as was determined necessary for this project, was well suited for determination by method of Bayesian statistical analysis. And, as seen from previous work in the field of medical controls, verification of the overall effect of this project would be idyllically simple, as implementing this model with a controller and analyzing the variance would be enough to determine if there had been a sufficient change to the therapy given [15]. Thus, the next step would be to implement the Bayesian statistical methods in order to determine the required parameter values for the model, i.e. set equation.

To implement Bayesian statistics, we utilized the open-source WinBUGS software package, run through the R programming language. By analyzing the confidence interval data for each parameter, and the chi-squared value for the model overall in the log files produced by WinBUGS, it was possible to determine if the model configuration and generated parameter sets were correct, or that the current model needed to be rethought.

The most important aspect of WinBUGS was its application of Markov Chain Monte Carlo integration (MCMC). It is the MCMC which performs the calculations necessary to determine the posterior distribution for  $\bar{\theta}$ ,  $p(\bar{\theta}|y)$ , and thus allows the user to determine the updated model parameters. MCMC is necessary as often it is not easy, or even necessarily possible to determine the correct conjugates required for the integration which can be seen in (1.3) [14].

$$E[\bar{\theta}|y] = \int_{\bar{\theta}} \bar{\theta} p(\bar{\theta}|y) d\bar{\theta} \quad (1-3)$$

Where  $E[\bar{\theta}|y]$  is the expectation of the parameter set given the values  $y$ ,  $\bar{\theta}$  is the parameter set, and  $p(\bar{\theta}|y)$  is the posterior distribution of the parameter set. As previously stated, it is the application of MCMC which in the case of a multi-parameter problem, solves the issue of identifying a conjugate prior. This is necessary as with an increase in the number of parameters, there is also an increase in the difficulty of determining a conjugate probability. Here, a conjugate probability refers to the integral equation which is a closed-form expression of the posterior, i.e. an expression which yields the values of  $p(\bar{\theta}|y)$ . Therefore, the use of MCMC prevents, or solves, the problem of having to deal with difficult integration altogether. It is also important to note that generally, a joint

posterior distribution is of a nonstandard form for an arbitrarily large parameter set, in which case the user would have no other suitable option than to apply MCMC [14].

The method employed by WinBUGS to implement MCMC is Gibbs sampling. Gibbs sampling is a special case of the Metropolis-Hastings algorithm which will generate the Markov chains by splitting the parametric vector  $\bar{\theta}$  into sub-vectors which are each sampled conditionally on the most recent values of all other  $\bar{\theta}$  parameters [14]. This essentially means that each individual model parameter is sampled based on every other model parameter at any given time, allowing there to be a more accurate predicted value of the sampled parameter.

The algorithm of Gibbs sampling is as follows [14]:

1. Chose an arbitrary value for each parameter of  $\theta$ . (here super-scripts represent iteration)

$$\theta = \{\theta_1^0, \theta_2^0 \dots, \theta_k^0\} \quad (1-4)$$

2. Sample new values for each parameter by cycling through the following:

- A. Sample a new value for  $\theta_l$  from the full conditional distribution of  $\theta_l$  given the most recent values of all other parameters and the data set:

$$\theta_1^1 = p(\theta_1 | \theta_2^0 \dots \theta_k^0, y) \quad (1-5)$$

- B. Sample a new value for  $\theta_2$  from its full conditional distribution given the most recent values of all other parameters and the data set:

$$\theta_2^1 = p(\theta_2 | \theta_1^1, \theta_3^0 \dots \theta_k^0, y) \quad (1-6)$$

Note:  $\theta_l^1$  is included instead of  $\theta_l^0$  since it is the most updated version.

- C. Repeat for all  $k$  parameters.

This completes one iteration of the Gibbs sampler and generates a new iteration of the parameter set  $\bar{\theta}^l$

3. Repeat step 2 for many iterations to obtain a sequence of dependent realizations of the parameter set  $\bar{\theta}$ .

Due to the functionality of Gibbs sampling the full conditional distribution which allows the updated parametric information to be obtained can often be reduced to a distribution specific random number generational method, thus reducing the overall complexity of the entire process considerably [14]. Such an implementation was utilized in this project, following an assumed normal distribution for each parameter.

## **CHAPTER 2**

### **MATERIALS AND METHODS**

#### **2.1 Experimental Setup**

All experiments were performed using BALB/c mixed gender mice. The care and handling of mice followed the Louisiana Tech University Institutional Animal Care and Use Committees protocol. Prior to injection, each mouse was kept under specific temperature control (35-39°C) to facilitate intravenous cannulation and to maintain consistency with drug delivery protocols designed to promote perfusion. Isoflurane inhalation (3% for induction and 2% for maintenance) anesthesia was used to immobilize a mouse during the injections; this aided in the collection of data [5].

#### **2.2 Injections of ICG in Mice**

A fresh ICG solution was prepared each day with a target concentration of 156 mg/mL which, according to Beer's Law ( $A = \epsilon cd$ ), has an absorbance of 300; the actual absorbance of ICG used varied from 197 absorbance to 318 absorbance. Stability of the solution at this high concentration necessitated the use of dimethyl sulfoxide (DMSO) (10% by volume) and spectrographic analysis to ensure that the peak at 780 nm was dominant in the stock solution [15].

ICG injections were given with the intent to reach one of three pre-specified points of maximum absorbance in the animal: small (2.25 absorbance), medium (3.00

absorbance), and large (3.75 absorbance). Each mouse was kept at approximately 36°C for the duration of the experiment in the presence of a space heating fan, and placed on a heating pad set to that temperature. The injections were carried out intravenously via tail vein using a custom catheter system fashioned from a 28 gauge needle tip and 2-french tubing. The method of injection was through a syringe pump (New Era Pump Systems, Inc. Farmingdale, NY. Model # NE-1010) which was programmed to inject the provided ICG solution at an initial rate of 15  $\mu\text{L}/\text{min}$ . During the course of all injections, the data was collected by the PPG data probe, placed near the base of the mouse's tail.

### **2.3 The Photoplethysmograph**

The PPG is a non-invasive optical monitoring device that can detect an optically active compound in the blood stream by measuring the optical extinction at three different wavelengths of light [16]. The PPG consists of an optical probe, analog signal modification circuitry and a LabVIEW DAQ which feeds all the received data into the created LabVIEW program for processing, monitoring, and cataloguing. Given the optical similarity of ICG dye to the nanoparticles for which the system was initially designed, the probe was implemented unchanged using optical extinction measurements at 660 nm, 805 nm, and 940 nm. This probe detects the pulsatile blood signal in a tissue mass and calculates the concentration of ICG according to AC805/DC [9].

When using the PPG, a strict inclusion criteria was maintained on all collected data. A data point was created by the system by averaging data collected over 5 seconds. The criteria for retaining each data point was that it had a standard deviation of less than 0.03 mV, that the mouse heart rate calculated from the observations of the three system

wavelengths each be within 20% of the computed mean heart rate, and that the voltage peak-to-peak of the AC portion be greater than 1.5 mV [11].

## 2.4 Bayesian Analysis

In order to implement the feedback control system with the PPG, it was necessary to first create the population model. The selected method for creating the population model for this study was Bayesian statistics. Bayesian statistics is the application of previously collected data to statistical models as a method of enhancing and adapting the accuracy of the models. This can be rephrased in more technical terms to mean that Bayesian statistics allows the user to assume a certain statistical distribution exists for a given random variable, and then update that distribution with observed knowledge, i.e. adapt and update the model with the new information [14]. In doing so, it lends itself well to the method of creating population models, in which case the model parameters would generally be taken to be random variables. It should be noted that this is contrary to the frequentist statistical analysis in which the data are considered to be random variables and the model parameters are considered to be unknown set values [14]. This means that by applying Bayesian statistics to model creation by collecting new information from individuals of a population the model may be updated for a better fit to the population.

The version of WinBUGS used in this study was 1.4.3. This was implemented with R version 3.1.2. The R packages used in this implementation were R2WinBUGS, coda, lattice, and MASS. To determine the fit of the model to a given parameter set the chi squared value was observed, this represents the variance of the variance of the model system and is a good indicator as to the overall outcome of an analysis. Using this chi

squared value it was possible to determine if the model was an over-fit, as was discovered early in the project when an initial two compartment model was being implemented.

## CHAPTER 3

### PHARMACOKINETIC MODEL IDENTIFICATION

#### 3.1 The Population Pharmacokinetic Model

Pharmacokinetics is the study of how therapeutic agents are changed by a body or system, population pharmacokinetics is the application of this study with the intent of generalizing the outcome a population of organisms will have on a specific therapeutic agent. Thus population pharmacokinetics was ideal for implementing a set equation for the controller used in this study. The population pharmacokinetic model was identified by comparing the absorbance versus time data and pharmacokinetic model predictions using the WinBUGS software. The covariate free one compartment model structure selected for use in this study was determined by observing the deviance information criterion of different pharmacokinetic models. The following model components were evaluated: inter-mouse variability and inter-trial variability on clearance (the rate at which a body removes a therapeutic agent) and volume of distribution (the effective volume which a given therapeutic agent may reach within a body); additive, proportional, and combined residual error models; and covariate effects of heartrate, O<sub>2</sub> (Oxygen) level, and mouse weight on clearance and volume of distribution. A non-informative normal distribution was used as the prior distribution for these pharmacokinetic model

parameters. Inverse gamma distributions were used for the precision of normally distributed error [11].

The one compartment model, given by (3.1) or (3.2), provided an excellent fit to the available data based on the measured absorbance. The concentration of the therapeutic agent in the mouse bloodstream was available in the form of experimental data from the PPG [11].

$$\frac{dA}{dt} = -\frac{CL}{V}A + \frac{RATE(t)}{V}; \quad A(0) = \varphi_0 \quad (3-1)$$

$$A(t) = \left[ \frac{-RATE(t)}{CL} \right] e^{-\frac{CL}{V}t} + \frac{RATE(t)}{CL} + \varphi_0 \quad (3-2)$$

In equations (3.1) and (3.2)  $A(t)$  is the absorbance (as an analogue for concentration),  $CL$  is the clearance rate,  $V$  is the volume of distribution,  $\varphi_0$  represents the absorbance shift from baseline due to PPG system noise,  $RATE(t)$  is the injection rate over time, and  $t$  is time. These variables correspond to the basic theory in chemical engineering of the extinction of a one compartment system with a given input concentration of an external solution. As such they correspond to the same concepts as within the pharmacokinetic model, where clearance rate is the rate of flow of the base fluid of the compartmental system, volume of distribution is the volume which the input solution may theoretically extend to within the compartment, or theoretically the volume of the compartment itself, and rate corresponds to the inflow rate of the input solution. It is interesting to note how similar this system ideology is to the analog in electrical engineering involving a single pole filter.

An ICG pharmacokinetic model for BALB/c mice was identified based on concentration versus time measurements from the PPG for a total of 22 injections divided

into three injection size categories: small (7 injections), medium (9 injections), and large (6 injections) using 8 BALB/c mice (see **Figure 3-1**).

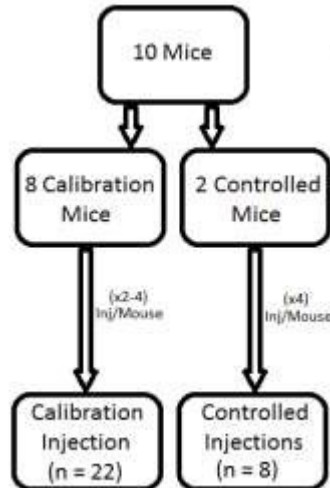


**Figure 3-1:** Flow chart describing distribution of mice within experimentation parameters.

Once the final population pharmacokinetic model was identified, we used the posterior distribution of parameters from WinBUGS as the population model parameters defined above. In other words, the values of  $CL$ ,  $V$ , and  $\varphi_0$  were determined through WinBUGS in the manner described in section 1.5 wherein they constituted the components of a parameter vector,  $\bar{\theta}$ , as described in equation (1.4). It was these parameters that are applied to the pharmacometric model set equation (3.2) for developing the control system.

## **CHAPTER 4**

### **CONTROL SYSTEM AND TUNING**

#### **4.1 Selected Control System**

In this study a form of PID controller was selected for use with the system. This was because of the overall ease of implementing a PID style controller. A PID controller needs only to be properly tuned and then provided the error signal produced by the system which it is controlling. Had this study used another form of control, it would have been necessary to design the controller from the ground up, which can be a tenuous process in itself. The most important aspect of designing a controller is verifying its stability, which is systematically possible, but can become extremely difficult depending on the required components of the controller. Overall to avoid such complications, as this study more focused on a proof-of-concept approach to the application of control theory to a medical treatment, a form of PID controller was selected for use with this project.

A proportional-derivative (PD) control system was used to control the error between the pharmacokinetic model predictions (the set equation) and the current concentration measurement (system signal). This PD system is a reduction of a proportional-integral-derivative (PID) control design. This reduction from PID to PD was used because the integral term may get quite large if the error term is never allowed

to go to zero. This is due to the fact that the integral term sums the error for all of process run-time [17]. Therefore, as this was a medical system designed with undershooting the set equation in mind it was beneficial to avoid using an integral term in the controller.

## 4.2 Control System Tuning

Although data points from the system were digital, not analog, the PD control system worked in much the same manner as would an analog PD control system: it numerically differentiated the error signal rather than using the analog derivative. The PPG collected data once every 5 seconds so the signal was discrete rather than continuous. This influenced the controller because the error signal was discrete as well. We used a continuous time solution to the differential equation for the set equation and then input the current time index of the received PPG data from the injection. This avoided any discrepancy between the analog-discrete setup we created because it allowed the analog differential equation to be used at the discrete points of data. As seen in the (4.1), the system error,  $e(t)$ , is calculated and used by the PD error equation.

$$u(t) = k_p e(t) + k_d \frac{de(t)}{dt} \quad (4-1)$$

The values  $k_p = 124.56$  and  $k_d = 48.91$  were obtained using the Zeigler-Nichols tuning rule, where  $u(t)$  is the controller [18]. The controller was operated based on a bang-bang principle. This means when the system was operating within its bounded margin of error, i.e. the current value of absorbance (OD) was within 30 % of the set equation  $A(t)$  (3.2) based on the value of  $u(t)$ , no action was taken by the adjustment equation, and conversely when the system was operating outside this bound based on  $u(t)$ , an adjusted rate was calculated following (4.2) algebraically.

$$RATE_{i+1} = 15 + \left( \frac{A(t_i + 1/15) - \alpha_i}{C} \right) * 4000 \quad (4-2)$$

In (4.2)  $RATE_{i+1}$  represents the next value of the injection rate in microliters per minute,  $15$  represents the base injection rate which the model assumes, i.e. 15 microliters per minute,  $A(t)$  is the absorbance equation seen in (3.2),  $\alpha_i$  represents the actual value of absorbance last measured by the PPG at time  $t_i$ , the  $+1/15$  term is used to calculate the PPG measurement at the next discrete time point, and  $C$  is the measured concentration of the stock solution of ICG being used in the current injection. The  $4000$  term is used to adjust the delta y calculation from absorbance to units of microliters per minute.

Traditionally a controller is implemented in such a way as to directly influence the system, not in following the method of bang-bang; equation (4.3) describes this operational methodology as it applies to this project.

$$RATE_i = RATE_{i-1} + u(t); RATE_0 = 15 \frac{\mu L}{min} \quad (4-3)$$

In (4.3)  $RATE_i$  represents the current value of the injection rate in microliters per minute,  $RATE_{i-1}$  represents the last value of the injection rate in microliters per minute, and  $u(t)$  is the controller equation as seen in (4.1).

An important concern we held in developing a control system for use as a therapeutic device was the potential danger of an erratic or poorly tuned system to the patient. In the event the controller were to over predict and inject more than required of a therapeutic agent, the patient would be at risk of toxicity. Therefore, we developed the controller with an intentional negative bias to ensure we were below the population pharmacokinetic curve and reducing the risk of toxicity by turning off the pump if the measured concentration was above the target. This equation represents a linear

adjustment to the desired model value at the next time interval of measurement, and in essence represents the classical method of Euler  $y_{i+1} = y_i + dy$ . This was chosen as the method of updating the *RATE* variable as the system operation time is in the range of seconds. Such a rapid response time allowed the use of this simple method, and due to the fact that this project was mainly a proof of concept a simpler method was desirable for the practicality of implementation.

### 4.3 Control Software

The control software was the primary component for enacting the objective of this project: controlling the drug concentration with time. The control software was written in the Python programming language, version 3.3.0, and implementing the serial, numpy, matplotlib, tkinter, time, os, and math libraries - it controls the ICG injections based on the real time absorbance measurements from the PPG. The set equation implemented for the PD control system was the identified Bayesian population pharmacokinetic model. The system enacted its changes through use of serial communication with the injection pump, calculating a new injection rate based on the current system error. Displaying all available mouse data (heart rate, O<sub>2</sub>, absorbance, injection rate, and total volume injected), and allowing for emergency system stop, the software was self-contained; given a concentration of ICG and valid injection endpoint, the system would run the injection to completion, auto-stop the pump, and then continue monitoring after injection.

To validate that the control system could follow a desired concentration versus time profile, the tuned system with pharmacokinetic model parameters and the PD control values were set within the software. This was then applied to a total of 8 injections on BALB/c mice, generating the controlled set. These injections were

performed with 3 in the small, 3 in the medium, and 2 in the large target absorbance group. The data collected from these injections was used to determine if control based medication was a valid option in future treatments.

#### **4.4 Analysis of Controller**

The viability of the controller was demonstrated using the error between the measured absorbance of each data point and the corresponding population pharmacokinetic model prediction. The primary outcome was the reduction in variance in the average error between data points in the calibration injections versus the controlled injections.

## CHAPTER 5

### RESULTS

#### 5.1 Data Inclusion Criteria

The PPG absorbance measurements were verified using the standard data metric for the device; any collected data from experiments was held to this metric to ensure reduced variability. An example of this metric for an uncontrolled injection is in the test output in **Figure 5-1**. These inclusion criteria are the following: average together the three values for heartrate obtained from each of the three wavelengths (660 nm, 805 nm, and 940 nm), and ensure an individual data point has its heartrate values within 20% of this mean heartrate, if not discard the data point. Next, measure the AC signal amplitude of each heartrate signal, and ensure they are between 1 and 100 mV. The final step in verifying the data is to ensure that no repeating data points are retained, as the PPG collects a new data point every 5 s, but records data every second, thus, the median data point in a 5 s collection group is selected and retained, this happens only if the others in its group of 5 s were not rejected following the criteria above, else that data point is also rejected. The applied inclusion criteria was developed by a previous project from this lab, when the PPG was developed for use with gold nanoparticles [16] (see The Photoplethysmograph subsection of Materials and Methods).

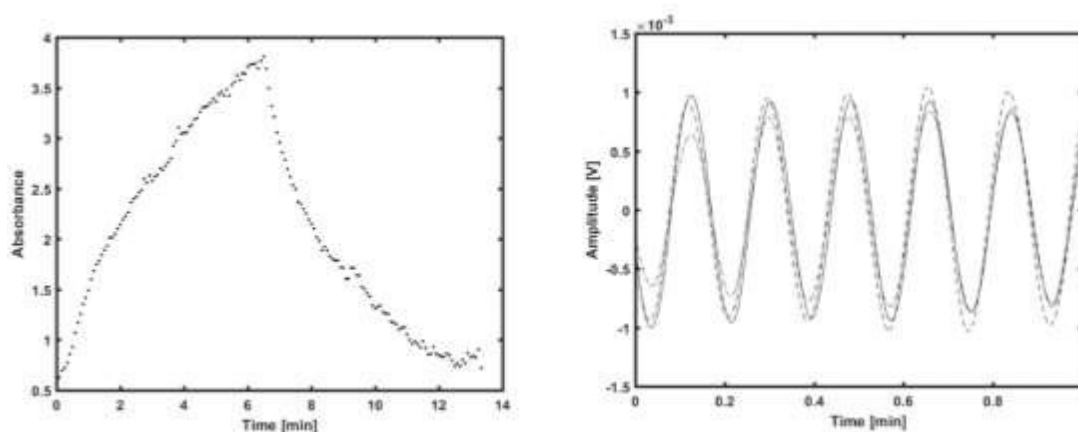


**Figure 5-1:** (Left) Example photoplethysmograph output of absorbance vs. time from mouse injection for an uncontrolled injection. (Right) Corresponding heartrate data from each wavelength (660 nm, 805 nm, and 940 nm) over a 1 min. interval.

## 5.2 Population Pharmacokinetic Model

A single compartment model provided an accurate and unbiased fit to the calibration data (22 injections performed on 8 mice at 3 maximum absorbance levels). This was verified following analysis of the chi-squared value from the output file, as mentioned in (2.4). There were no significant covariate effects on any of the model parameters. The resulting population pharmacokinetic model parameters are shown in **Table 5-1**.

**Table 5-1:** Population pharmacokinetic model parameters based on calibration trials (n=22)

<b>Median Parameter (95% Credible Interval)</b>		
Clearance	CL	1.10 (0.920 – 1.28) mL/min
Volume of Distribution	V	3.01 (2.69 – 3.34) mL
Shift	$\varphi_0$	0.663 (0.558 – 0.769)
<b>Inter Mouse Variability (95% Credible Interval)</b>		
Clearance	CL	0.412 (0.313 – 0.581) mL/min
Volume of Distribution	V	0.752 (0.568 – 1.07) mL
Shift	$\varphi_0$	0.241 (0.183 – 0.341)
<b>Residual Variability (95% Credible Interval)</b>		
$\sigma$	-	0.0906 (0.0884 – 0.0929)

The half-life from the calibration injections (1.89 min) agrees with a previously published report (2-4 min) [19].

### 5.3 Analysis of Controlled Injections

The primary outcome is that there was a 74.8% reduction in variance of the controlled group **Figure 5-2**. As can be seen, not only was the controlled group less varied on an individual basis of the injections, but the overall spread of the injection around the average was smaller as well. This data definitively displays the reduced variability of the controlled injections.

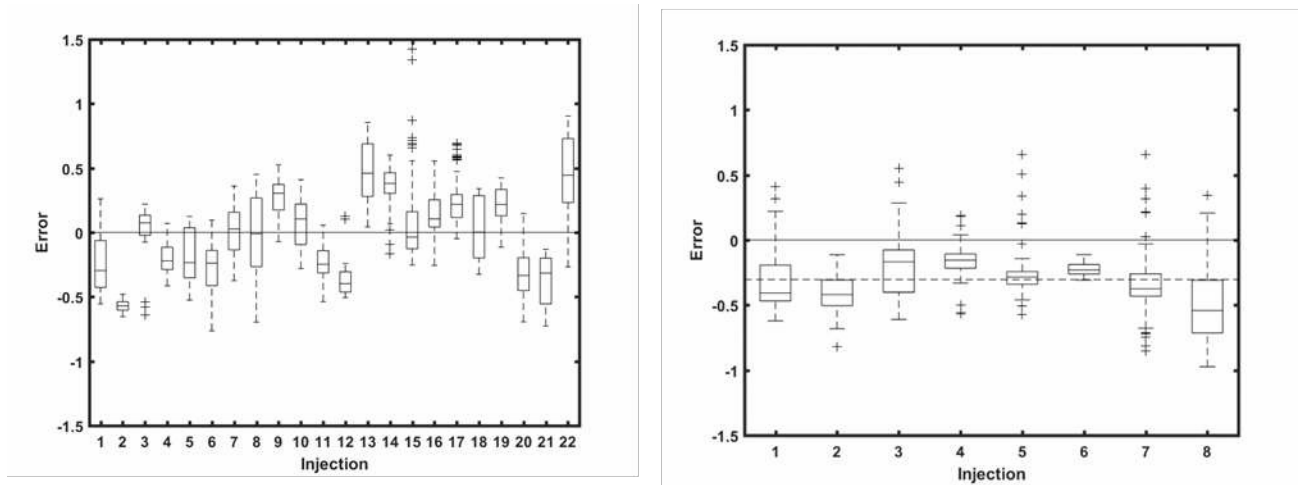


**Figure 5-2:** (Left) model comparison error of 22 injections from the controlled group represented as a standard box plot about the average (solid line) approximately 0. (Right) model comparison error of 8 injections from the controlled group as a standard box plot about the average (dashed line) approximately -0.3, calibration average (solid line) provided for comparison.

A demonstration of the controller in action can be seen in **Figure 5-3**. The system is corrected by increasing the injection rate when the measured concentration was below the target to better fit the provided target model.

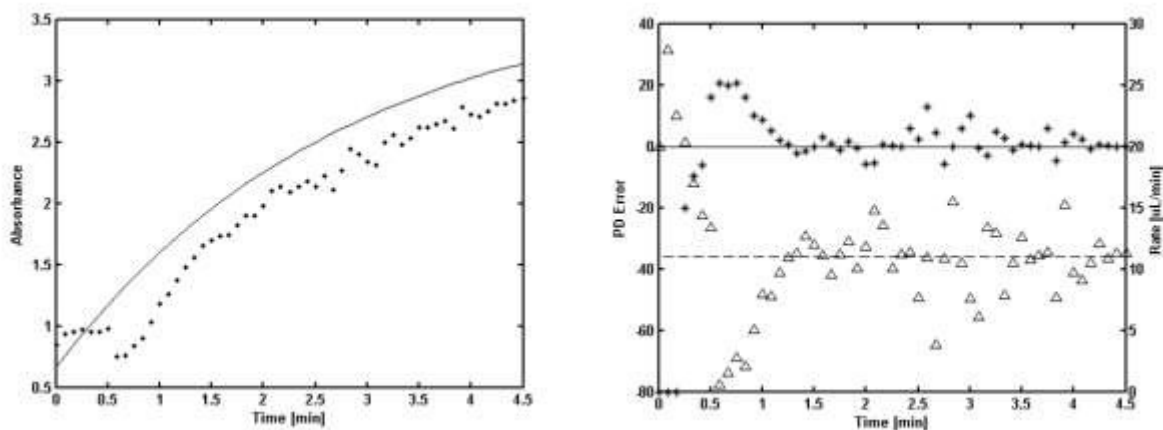


**Figure 5-3:** (Left) Example absorbance with time with injection control. (Right) Corresponding PD error and calculated injection-phase rate change. The dashed line is an asymptote of error (averaged) and solid line on left is the population pharmacokinetic model.

With the controller in place, we had a variance in the clearance rate comparable to that seen in the clearance rates and cardiac output metrics obtained in clinical studies employing ICG, using pulse dye densitometry [18, 19]. As seen in **Figure 5-4** the control group injections are displayed in comparison to the population pharmacokinetic model to represent this.

Because the goal of this project was the reduction in variability of injections of a therapeutic agent, we also analyzed the delivered dosage generated by the controller for each injection **Table 5-2**. While the control system may be given a certain termination point in time or absorbance, it was not calculating or using the area under the curve, or AUC, as is standard in many pharmacological studies. This is due to the systems feedback mechanism. Data collected by the PPG was optical absorbance, and therefore keeping the system simple and operating on this variable was ideal as this was only a proof of concept.

**Table 5-2:** Comparison between expected dose (Exp) and achieved dose (Inj) necessary to achieve a target absorbance in validation experiments.

Comparison between expected dose (Exp) and achieved dose injected (Inj) necessary to achieve a target absorbance in validation experiments								
Injection #	Target Absorbance	Stock Conc (mg/mL)	Exp Vol (uL)	Exp Time (min)	Exp Dose (mg)	Inj Vol (uL)	Inj Time (min)	Inj Dose (mg)
1	2.25	1.56	31.20	2.08	0.05	36.14	2.08	0.06
2	2.25	1.26	72.45	2.83	0.09	121.33	4.83	0.15
3	2.25	1.26	57.45	2.83	0.07	91.92	3.83	0.12
4	3.00	1.56	68.70	3.92	0.11	87.77	4.58	0.14
5	3.00	1.56	68.70	3.92	0.11	87.47	4.58	0.14
6	3.00	1.56	73.80	3.92	0.12	84.62	4.92	0.13
7	3.75	2.19	63.75	3.50	0.14	82.62	4.25	0.18
8	3.75	2.19	91.20	3.50	0.20	138.27	6.08	0.30

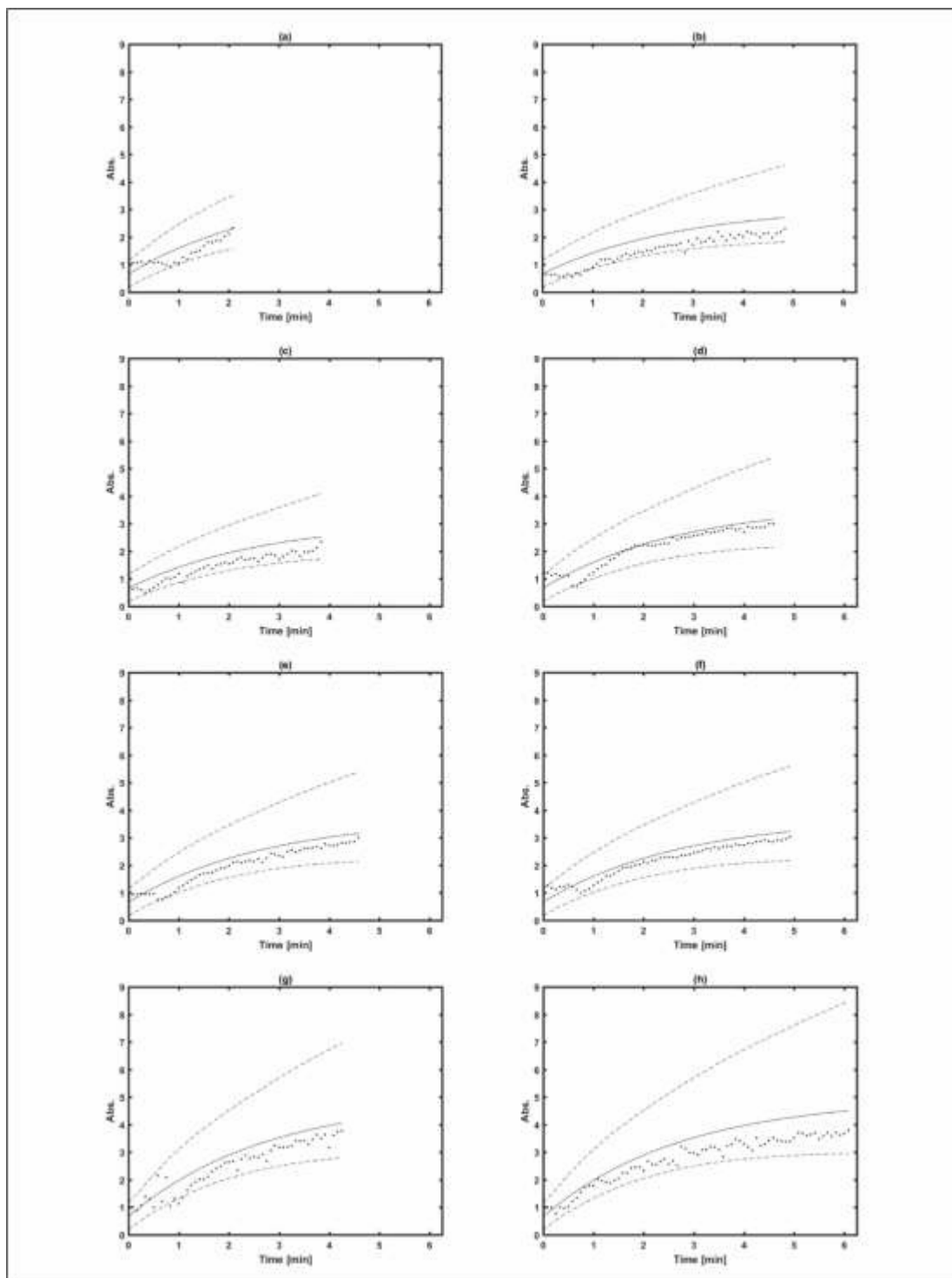


**Figure 5-4:** Injections from Controlled Data Set (dots) with target model (solid line) and 95% credible interval (dashed line), absorbance vs. time. Figures (a) – (c) have a final absorbance target of 2.25, figures (d) – (f) have a final absorbance target of 3.00, and figures (h) – (g) have a final absorbance target of 3.75.

## **CHAPTER 6**

### **DISCUSSION**

#### **6.1 Overview**

A population pharmacokinetic model was developed for the therapeutic agent ICG to study the feasibility of using a closed-loop PD control system for tracking a desired concentration profile during intravenous administration of drugs. We found that closed-loop control of ICG reduces variance from the target injection concentration profile by 74.8%.

#### **6.2 Controller Advantages**

There are several advantages to closed-loop control of injections for tracking a desired concentration profile. These are primarily due to the applied control system's application of system error when calculating the next move to make. For example, our approach has the potential to reduce acute toxicity by ensuring that the actual concentration is below the population pharmacokinetic model. Another example may be seen in the application of closed-loop control to a highly sensitive therapy. Take for example one which needs to be maintained in a tight therapeutic window for an extended period. Keeping the patient within this window is a considerably less difficult task as the system can be designed to maintain the window rigorously with the application of feedback control to the drug delivery system. Still another advantage seen in applying a

closed-loop control system is perhaps the most poignant caveat of control and automation systems in general. Control systems allow the designer to choose the operation and response time as well as the method and number of system reactions to a specific stimulus as relayed in the system error. Meaning, it is up to the designer in what way and how fast any form of system error is processed. Thus, the controller provides a more dynamic and robust platform upon which to expand any system. This cannot be accomplished without system feedback, and therefore cannot occur without the closed-loop.

### **6.3 Pharmacokinetic Observations**

In going from a target absorbance of 2.25 (Inj #1) to an absorbance of 3.75 (Inj #8) required 5 times the dose. Injection #1 appears to require a below average dose to achieve the desired concentration so the administration of the expected dose may lead to over-dose. On the other hand, Injection #8 required an above average dose to achieve the desired concentration so administering the expected dose may not be effective.

### **6.4 Controller Error Response**

The best case of this can be seen in the overall error response of the Controlled group, where the error is centered below the marginal average of zero. This is due to the system design. As previously mentioned considered the potential threat of therapeutic toxicity, we therefore implemented a negative bias as a precautionary measure. While this increases system response time, this has two benefits; it allows our system to run longer and therefore approach the asymptotic PD error margin of zero, as well as reduces the potential threat to the patient from a system malfunction caused by over injection.

## 6.5 General Outcome

Beyond this initial impact in reducing the variability of patient treatment, this study is an important step in the direction of fully-automated therapeutic systems. We demonstrate that the idea of self-sustained and self-controlled treatment systems is not only practical, but closer than other current work would seem to suggest. Overall, our study shows that interpatient variability need not influence the outcome of a clinical study, and by the same token, personalized medicine is in the near future.

## 6.6 Project Drawbacks

It should be noted that this study did not include the pharmacodynamics when considering our control system. This is reflected primarily in the choice of our style of control; i.e. a PD control system. Classically PID and all related modes of control are utilized in situations in which there are a plethora of unknown and or unmeasurable variables. The general idea behind a PID being to tune the error signal to a prespecified series of results in order to achieve the desired system convergence. In doing so, we focused entirely on meeting the goal of reduction of inter-patient variability and left all other system variation up to the control system. Thus, having designed our system around these aspects of the pharmacokinetics, no considerations had been made for the effect which the drug was having on the patients.

The main limitation is the system's undershooting of the population pharmacokinetic curve, though this is a measure to protect the patient from toxicity, (a potentially realistic concern in our overstepping of pharmacodynamics). In the future, a more finely calibrated control system, made with a more sensitive PPG, would not have this concern, and thus not need to undershoot. It should also be noted that the use of

absorbance as the target and general pharmacokinetic model standard in our study is not the clinical tradition.

Although this project focused on the use of optically-based controller feedback, the system need not have any specific type of sensory feedback. In future work, an exploration into other clinical metrics such as glucose, neurotransmitters, and hormone level therapeutic applications could be explored.

## **CHAPTER 7**

### **CONCLUSIONS**

#### **7.1 Future Work**

Controller based medical therapy is a new and developing field. As shown in our work it holds promise in reducing inter-patient variability. The future application of controllers to the many forms of medical treatment is the key to resolving the current issues held in the medical field which limit treatments based on small margins of population effectivity and will allow physicians to be more certain of the reliability of medical treatment overall. Such future works in this field might include the creation of a more compact version of the device utilized within this project, such that it might fit on a patient arm, containing all components of the described system within a smaller, closed-form casing, perhaps one that is 3D-printed to increase feasibility, reduce cost, and increase the device fit on an individual patient. Such a device might have a touch screen with a variety of options of therapeutic windows and/or treatment-session goals/outcomes, and would likely include a peripheral device worn at another location on the patient, such as the opposing wrist/appendage, to gain a more accurate measure of the administered drugs profusion. This hypothetical device need not focus solely on the application of optically-based feedback, but might also take measurements in similar form to a blood glucose monitor, or a manner similar or identical to radio therapy. This

hypothetical device would also likely not need to apply an undershoot or bias as was utilized in this project, and thus could potentially very tightly control the administration of its drug allowing previously toxic drugs to be safely administered. As can be seen from even one such theorized device, the future of control based medication holds potential as a means to broaden the availability of medical treatments to the global populous in a way that has yet to be available in the modern era.

## **APPENDIX A**

### **CALIBRATION DATA MODELS AND VALIDATION DATA**

The data used to develop the pharmacokinetic model, the calibration set, was analyzed on an individual basis. Each injection profile was modeled with a one-compartment pharmacokinetic model and in conjunction with properly determining the covariate effects which were potentially present, the heartrate of each mouse was also collected and graphed. This data is presented here, in Appendix A. Data was also collected during the validation experiments, for the purpose of future analysis and has also been included here, in Appendix A. A general note on the nomenclature used, M##I# in the below image captions represents which mouse number from a set, and which injection number for that mouse.

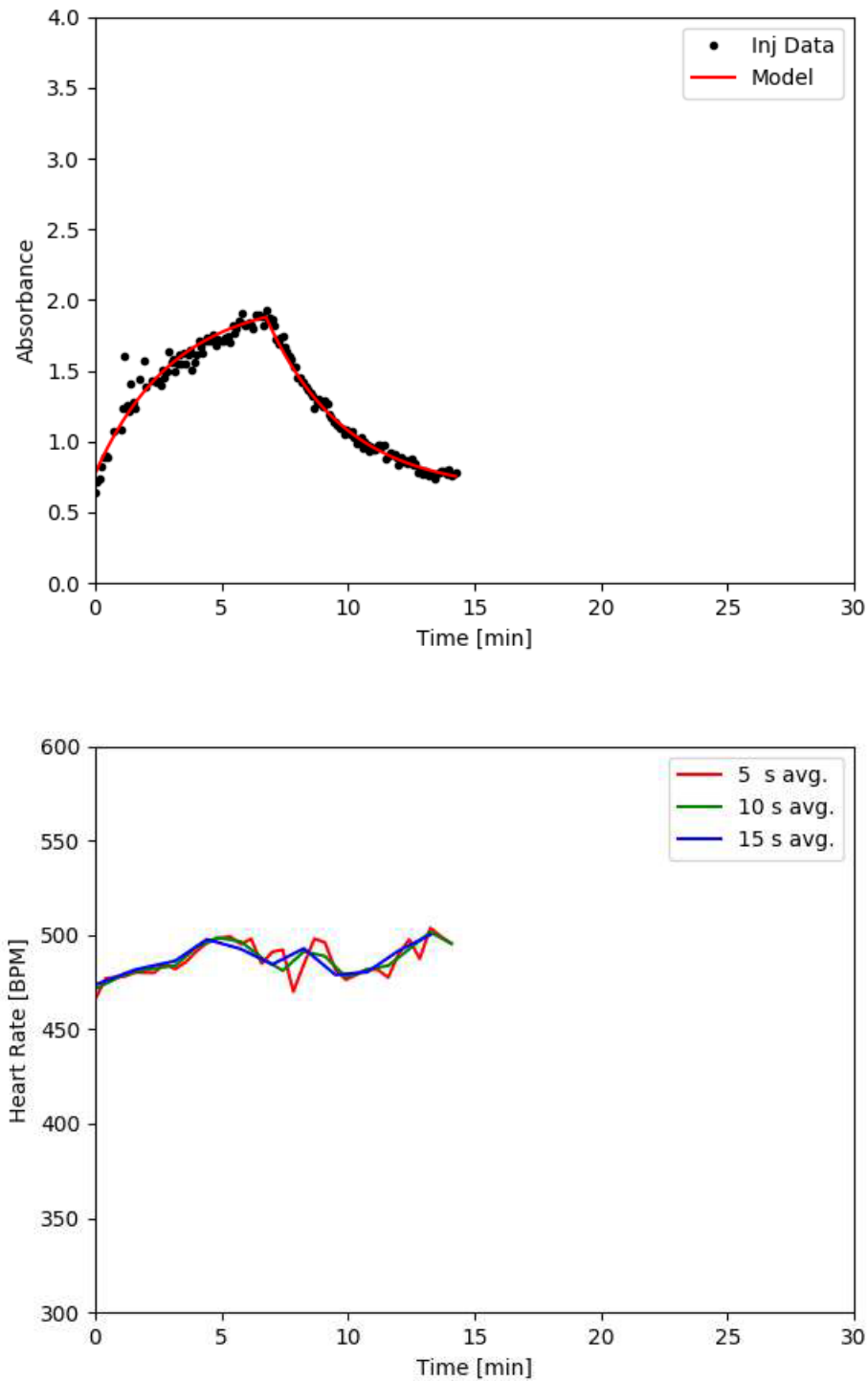


**Figure A-1:** (Top) Injection profile M1I1 (dots) with model (red line) and (bottom) heart rate data averaged over 5 (red line), 10 (green line), and 15 (blue line) seconds.

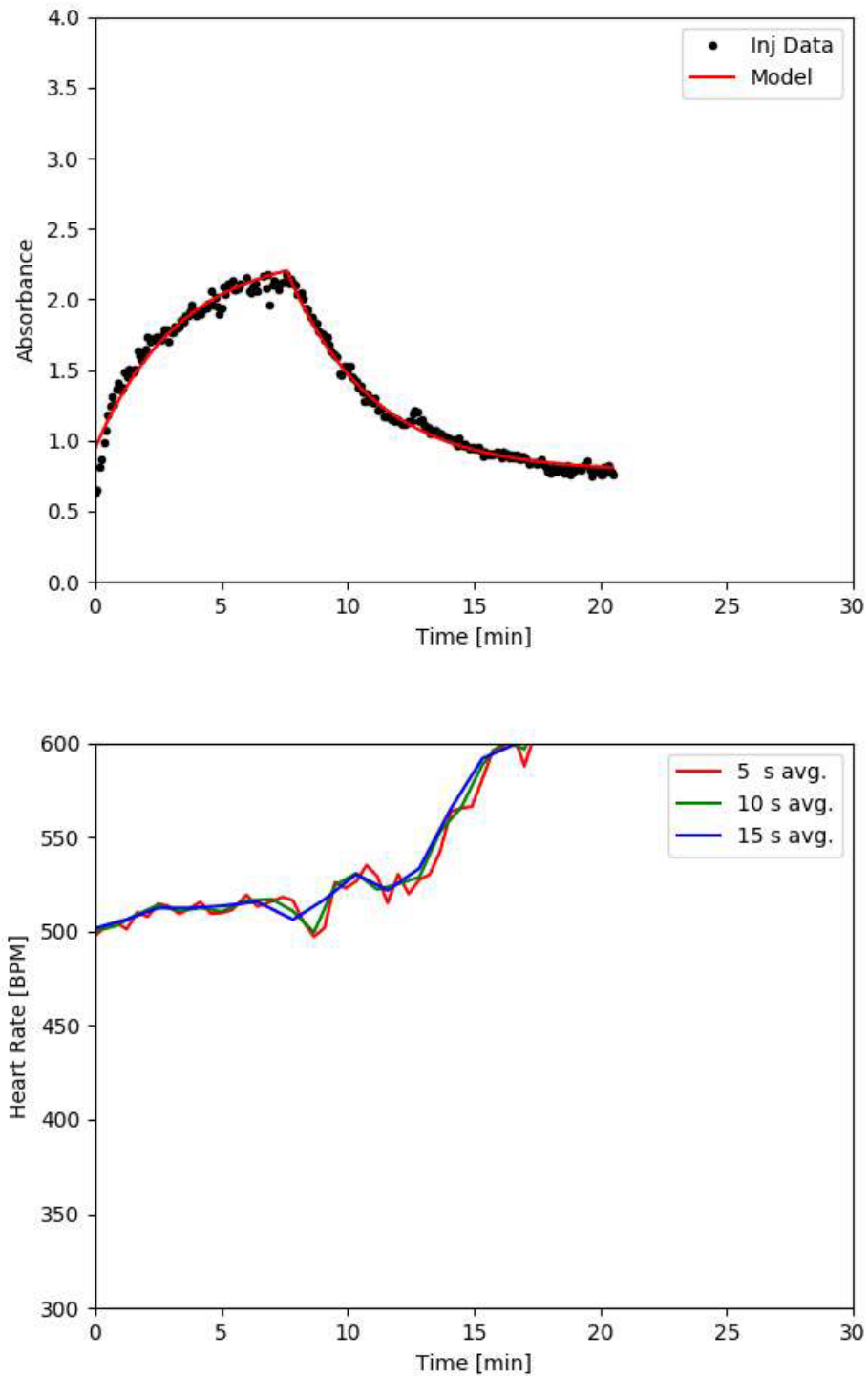


**Figure A-2:** (Top) Injection profile M1I2 (dots) with model (red line) and (bottom) heart rate data averaged over 5 (red line), 10 (green line), and 15 (blue line) seconds.

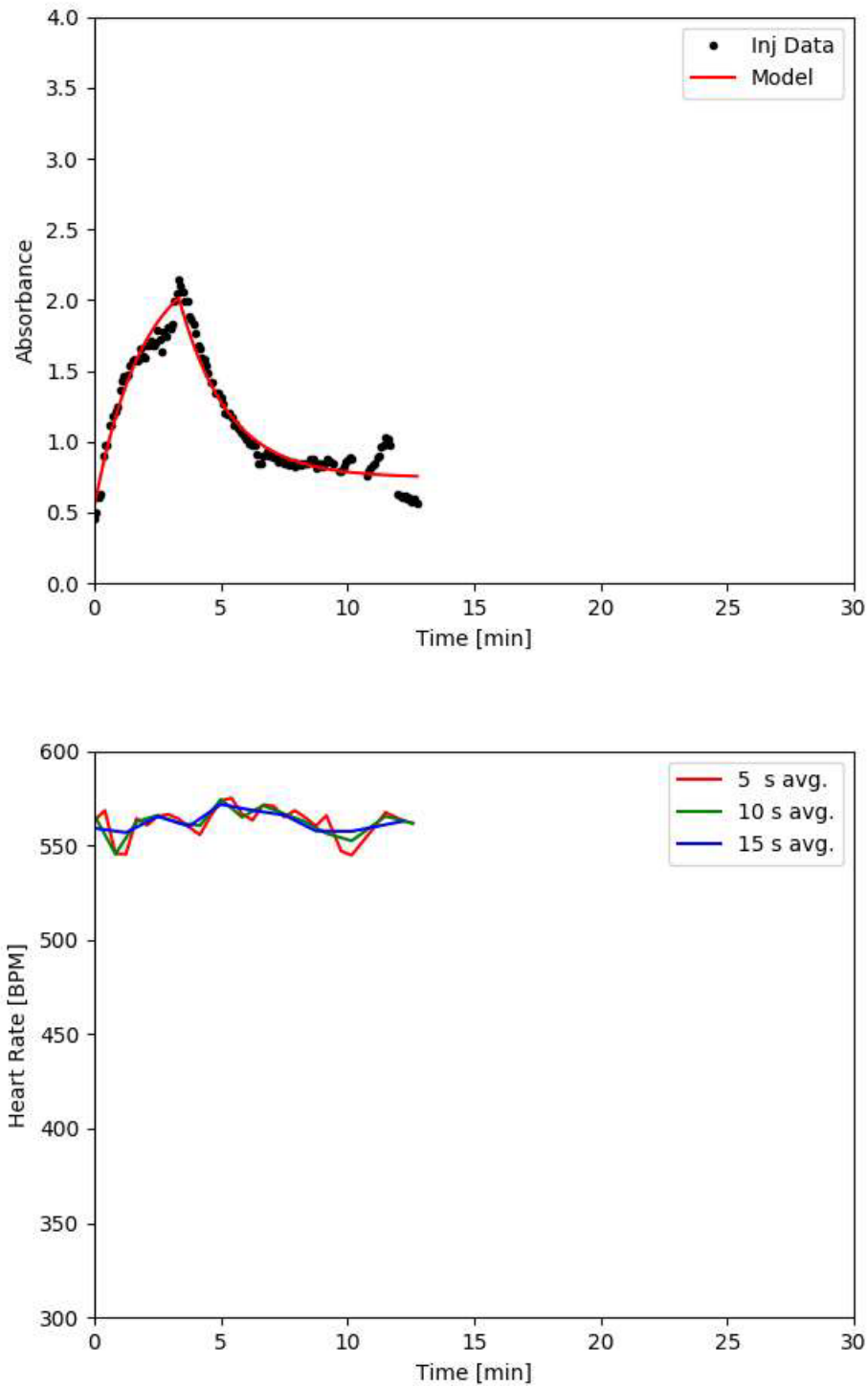


**Figure A-3:** (Top) Injection profile M2I1 (dots) with model (red line) and (bottom) heart rate data averaged over 5 (red line), 10 (green line), and 15 (blue line) seconds.

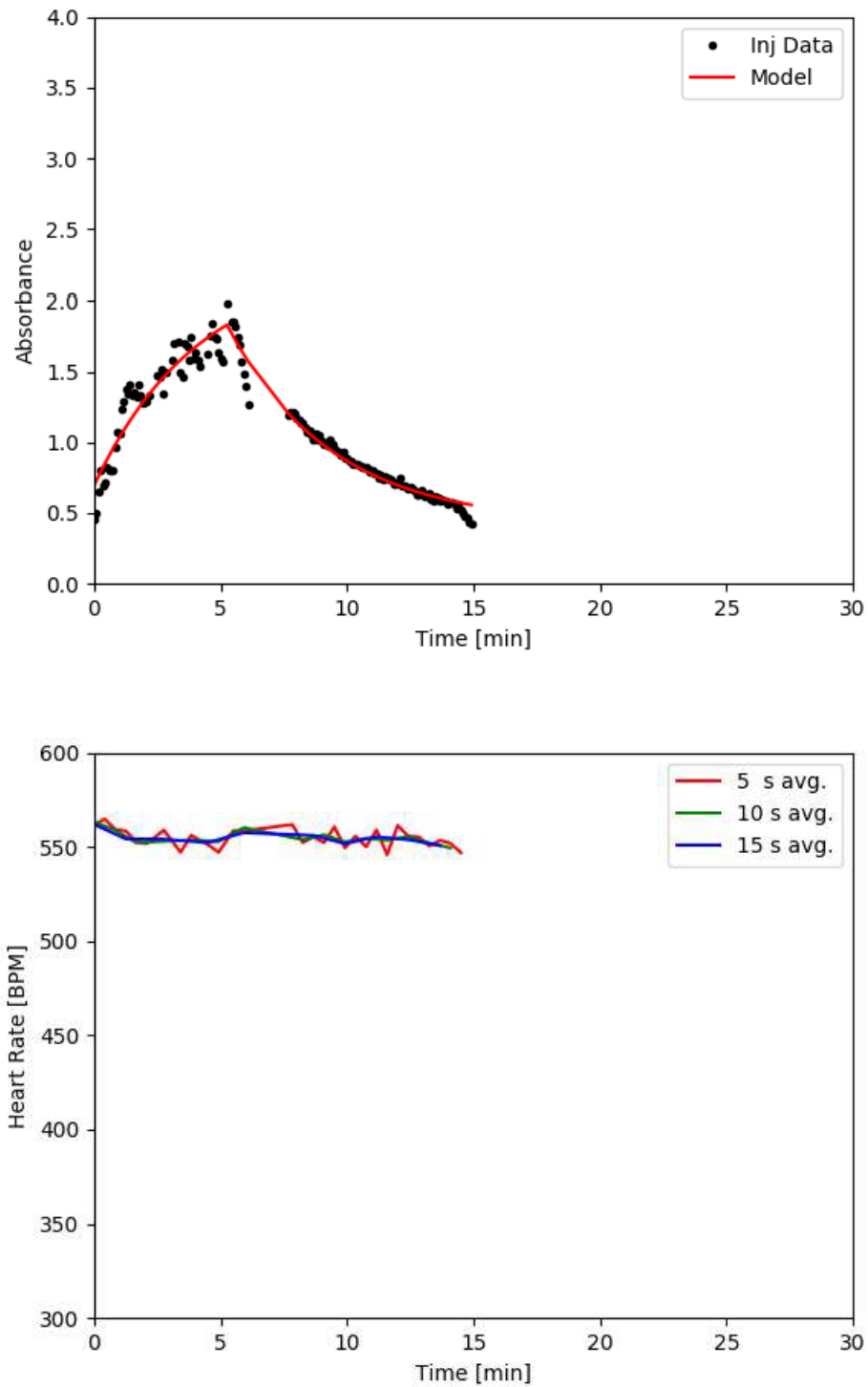


**Figure A-4:** (Top) Injection profile M2I2 (dots) with model (red line) and (bottom) heart rate data averaged over 5 (red line), 10 (green line), and 15 (blue line) seconds.

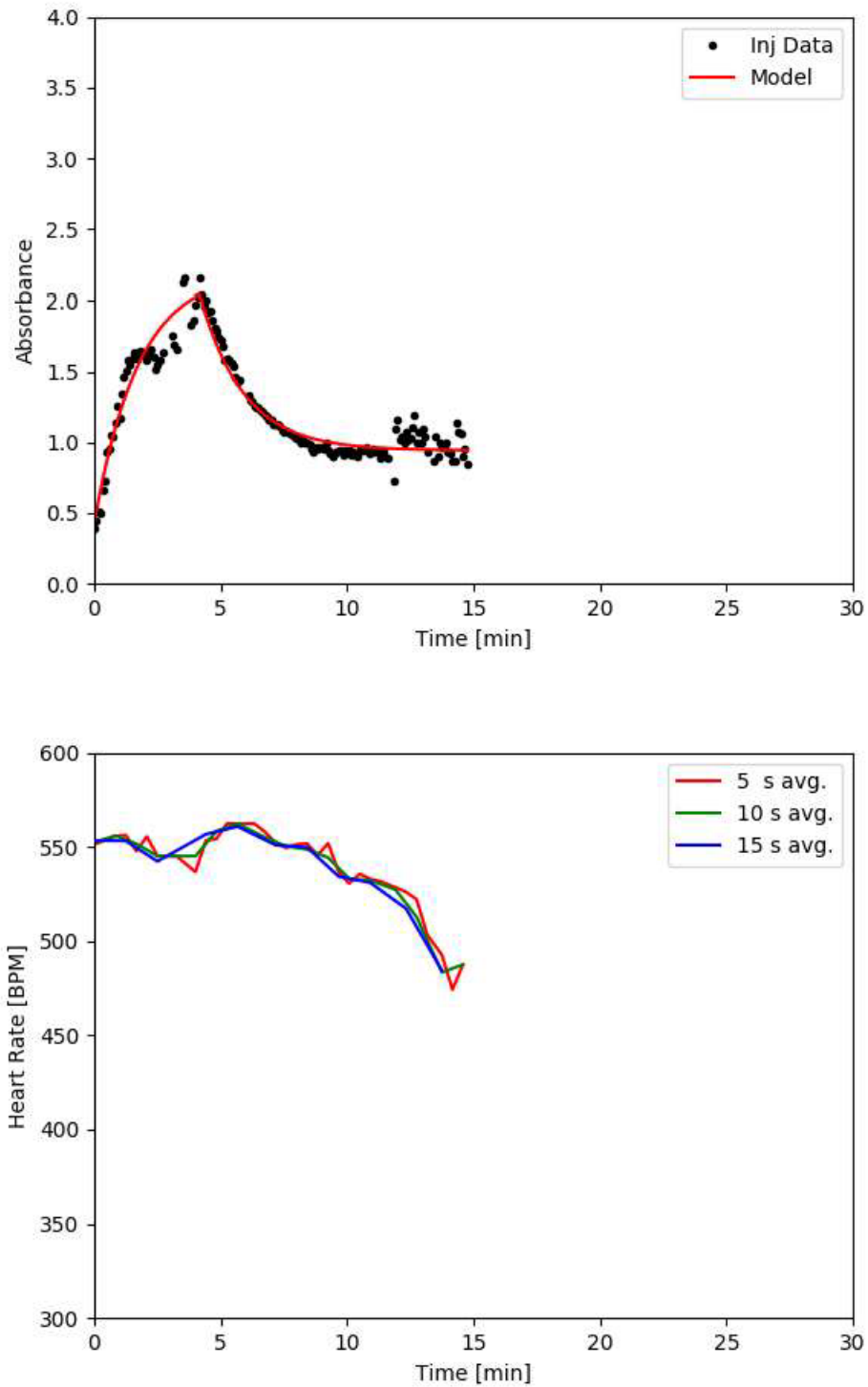


**Figure A-5:** (Top) Injection profile M2I3 (dots) with model (red line) and (bottom) heart rate data averaged over 5 (red line), 10 (green line), and 15 (blue line) seconds.

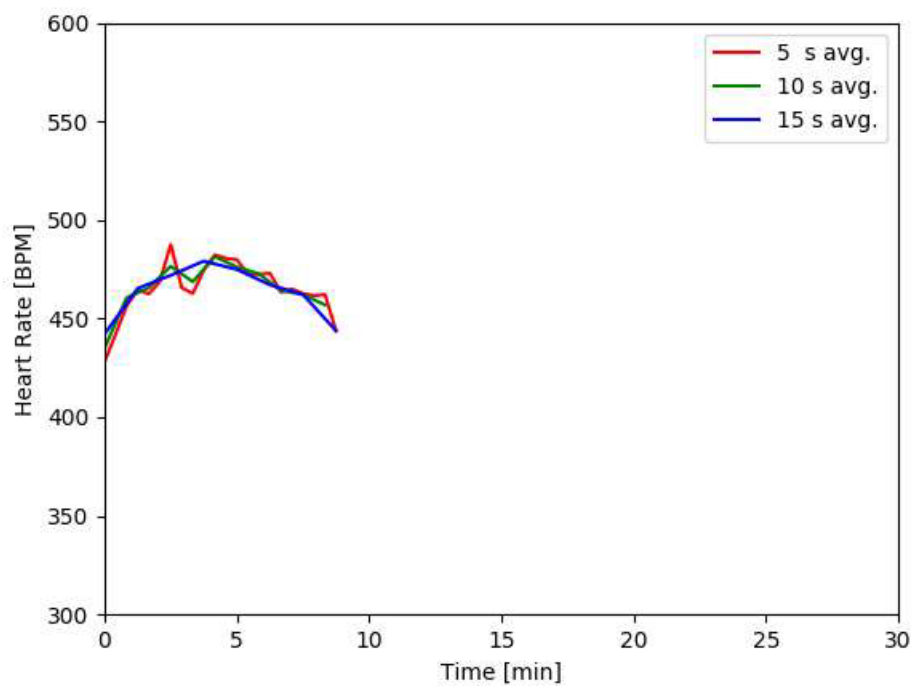
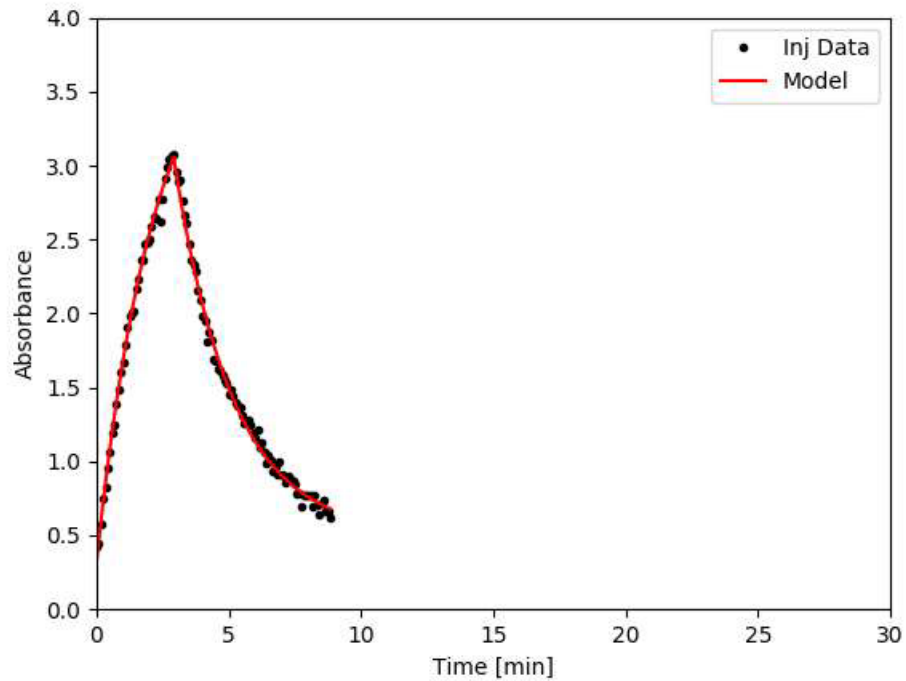


**Figure A-6:** (Top) Injection profile M3I1 (dots) with model (red line) and (bottom) heart rate data averaged over 5 (red line), 10 (green line), and 15 (blue line) seconds.

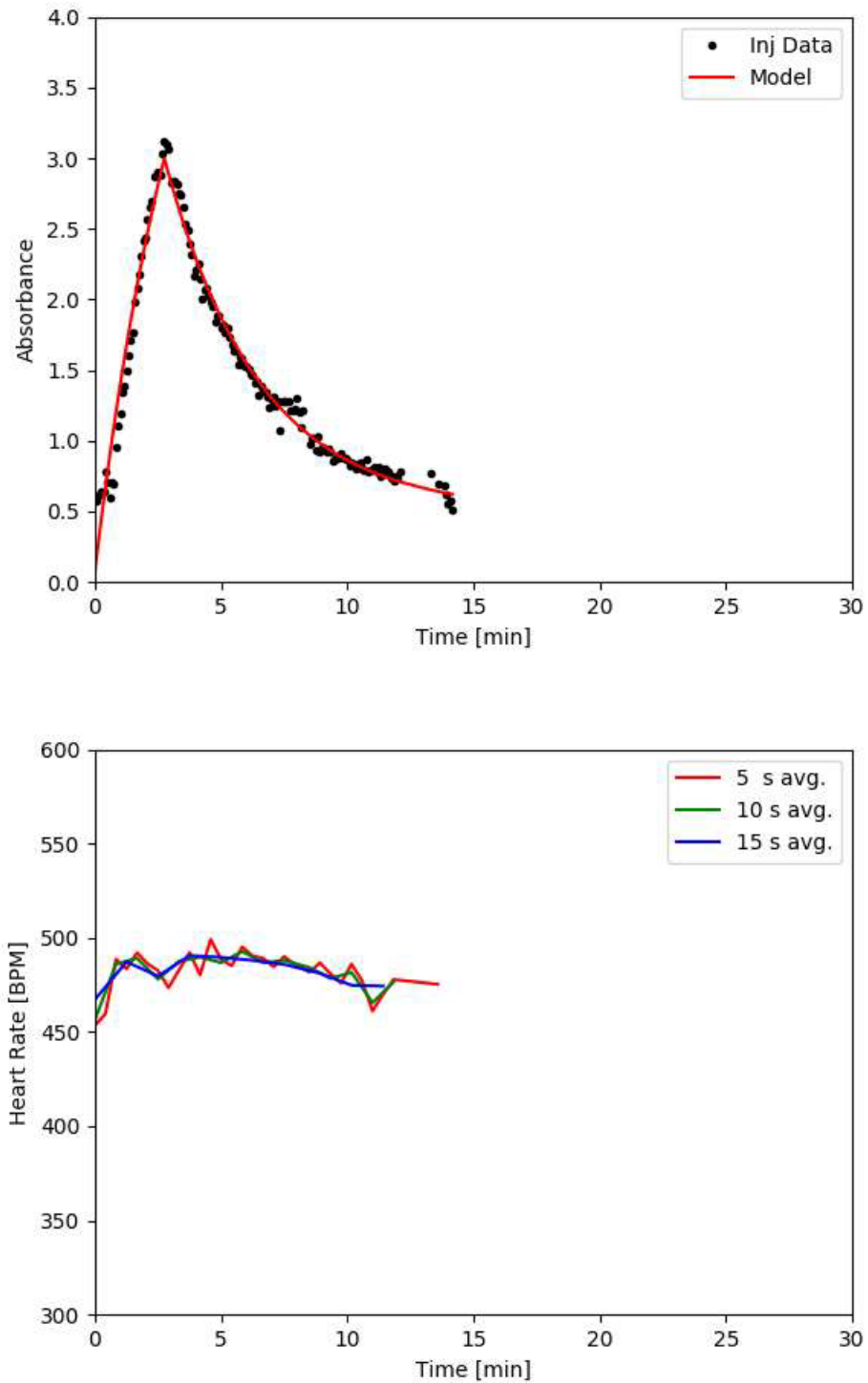


**Figure A-7:** (Top) Injection profile M3I2 (dots) with model (red line) and (bottom) heart rate data averaged over 5 (red line), 10 (green line), and 15 (blue line) seconds.

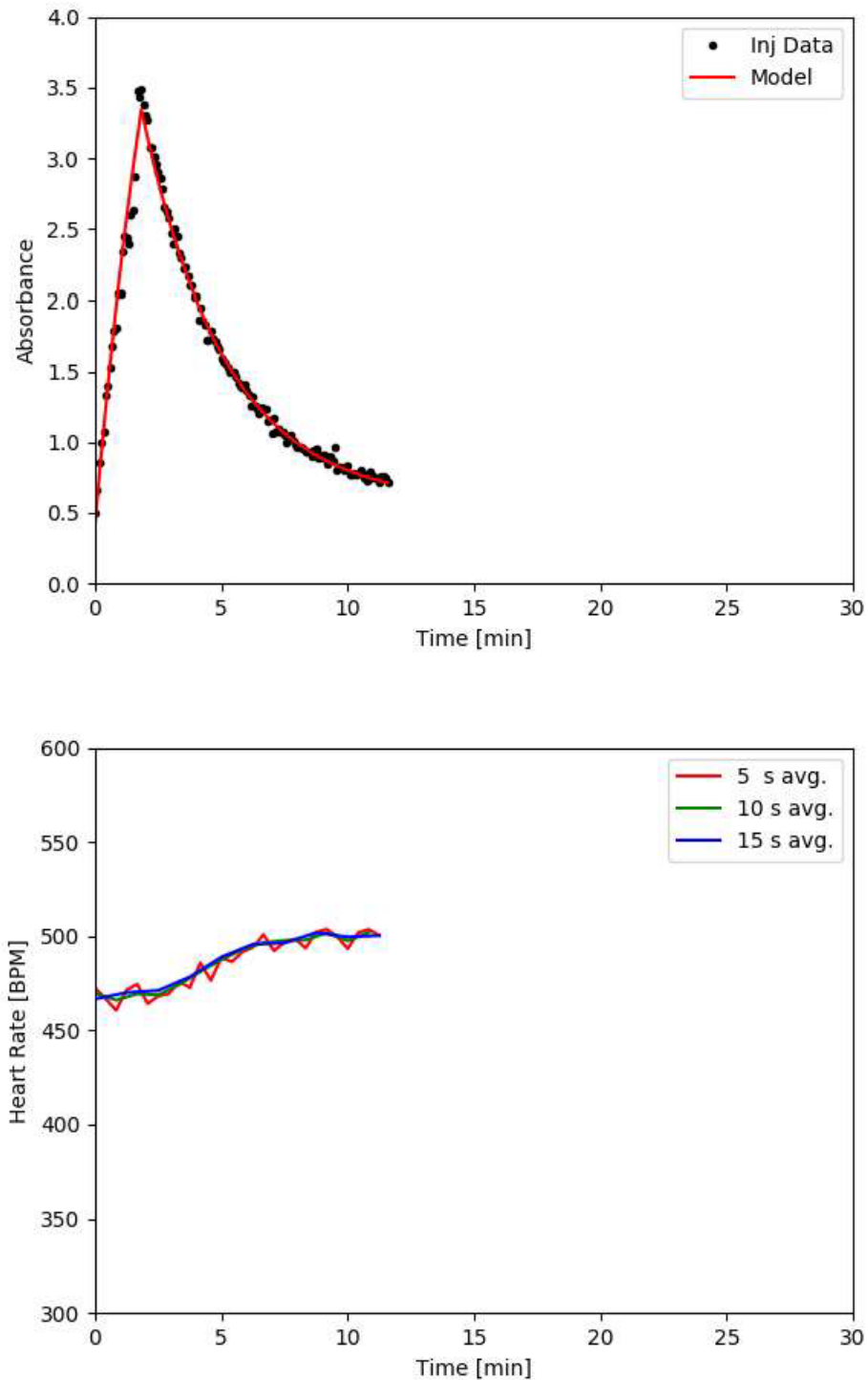


**Figure A-8:** (Top) Injection profile M3I3 (dots) with model (red line) and (bottom) heart rate data averaged over 5 (red line), 10 (green line), and 15 (blue line) seconds.

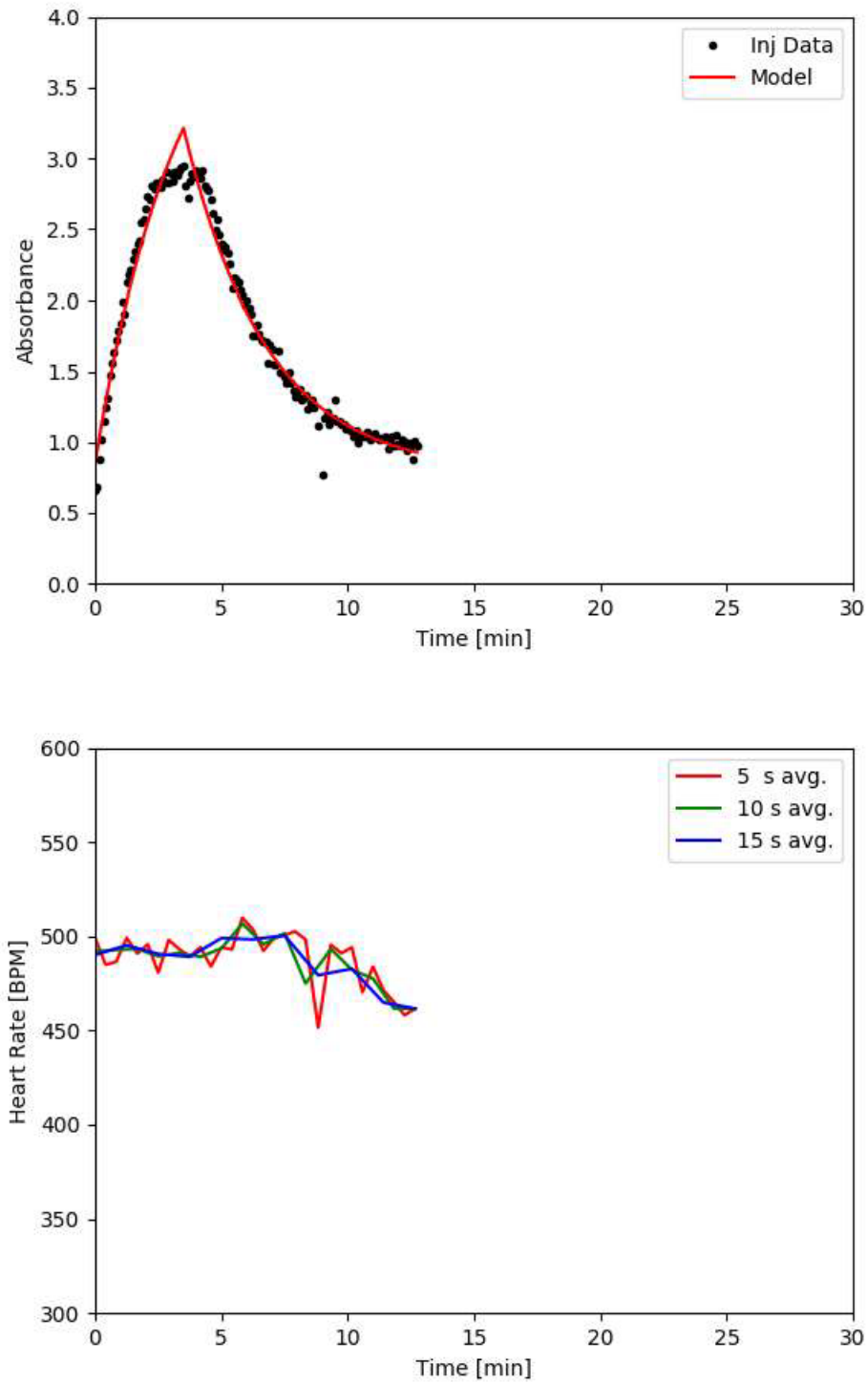


**Figure A-9:** (Top) Injection profile M3I4 (dots) with model (red line) and (bottom) heart rate data averaged over 5 (red line), 10 (green line), and 15 (blue line) seconds.

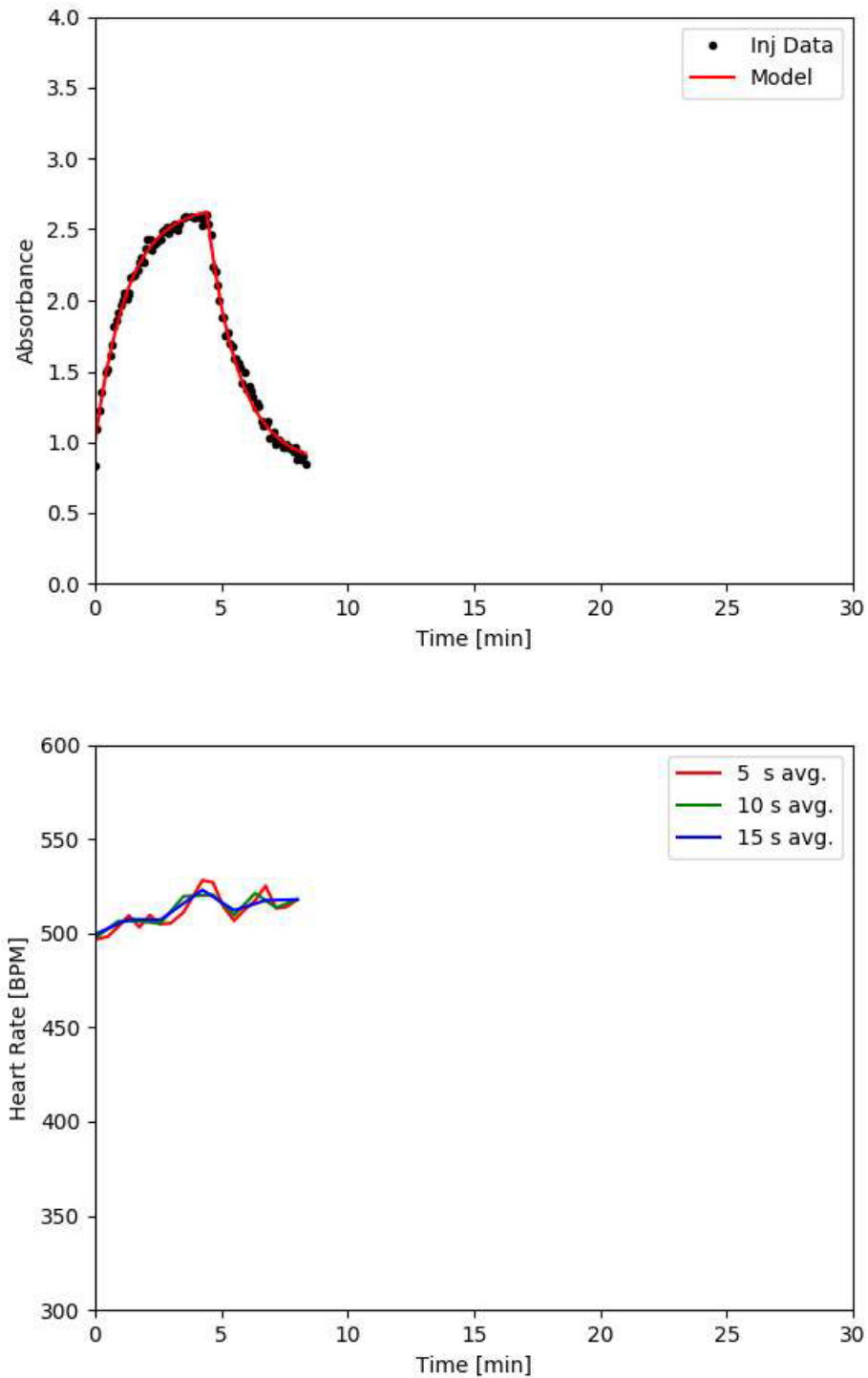


**Figure A-10:** (Top) Injection profile M4I1 (dots) with model (red line) and (bottom) heart rate data averaged over 5 (red line), 10 (green line), and 15 (blue line) seconds.

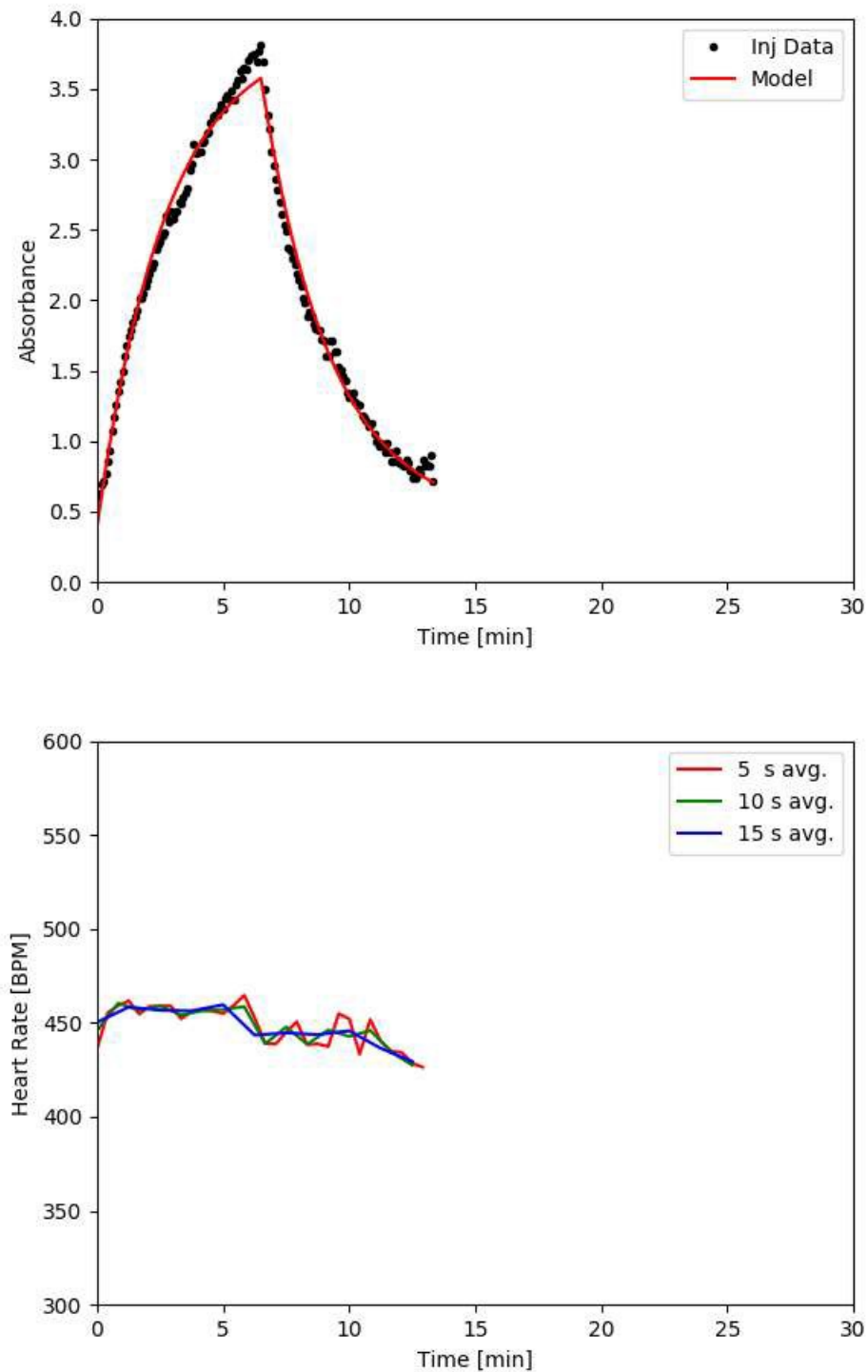


**Figure A-11:** (Top) Injection profile M5I1 (dots) with model (red line) and (bottom) heart rate data averaged over 5 (red line), 10 (green line), and 15 (blue line) seconds.

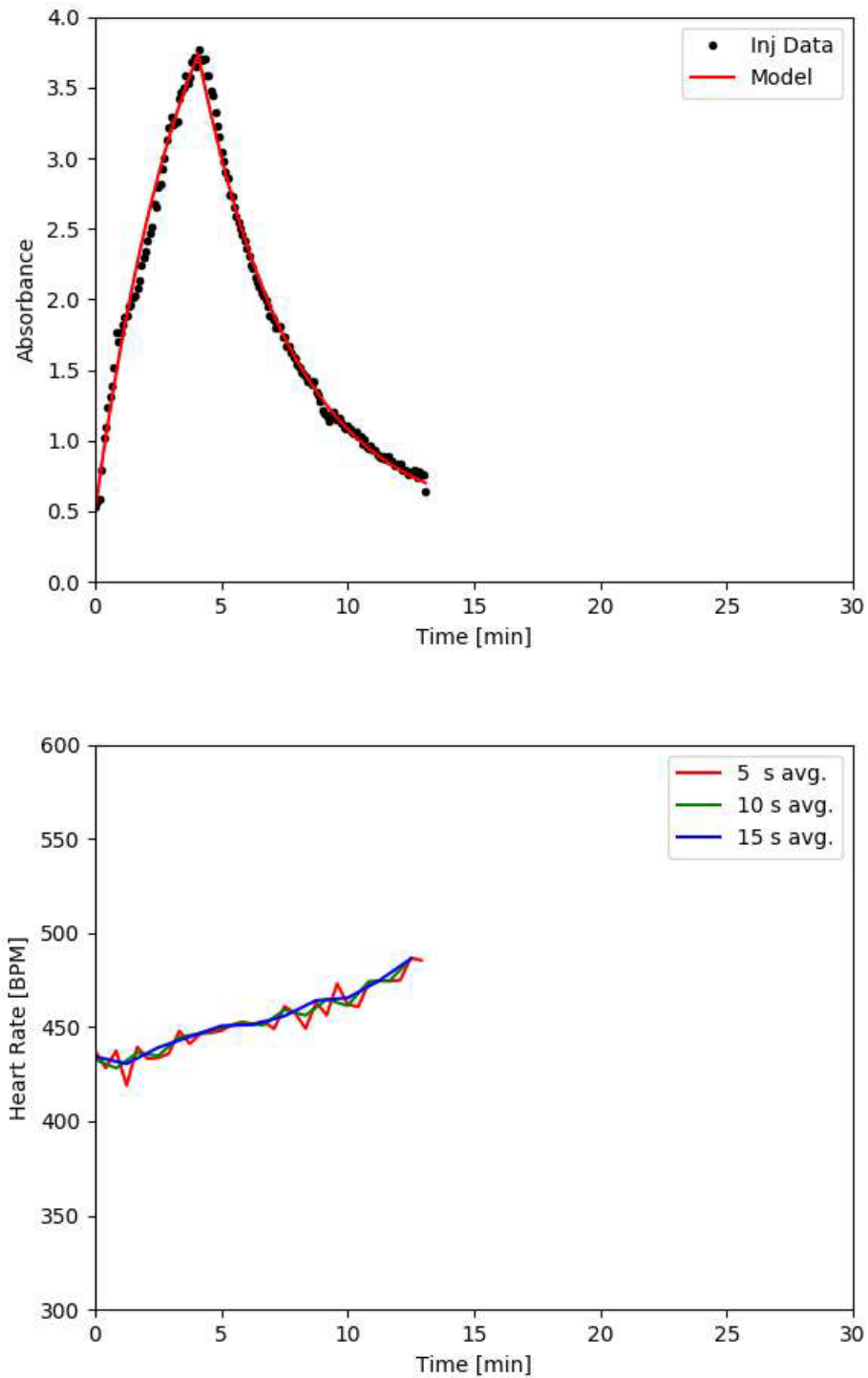


**Figure A-12:** (Top) Injection profile M5I2 (dots) with model (red line) and (bottom) heart rate data averaged over 5 (red line), 10 (green line), and 15 (blue line) seconds.

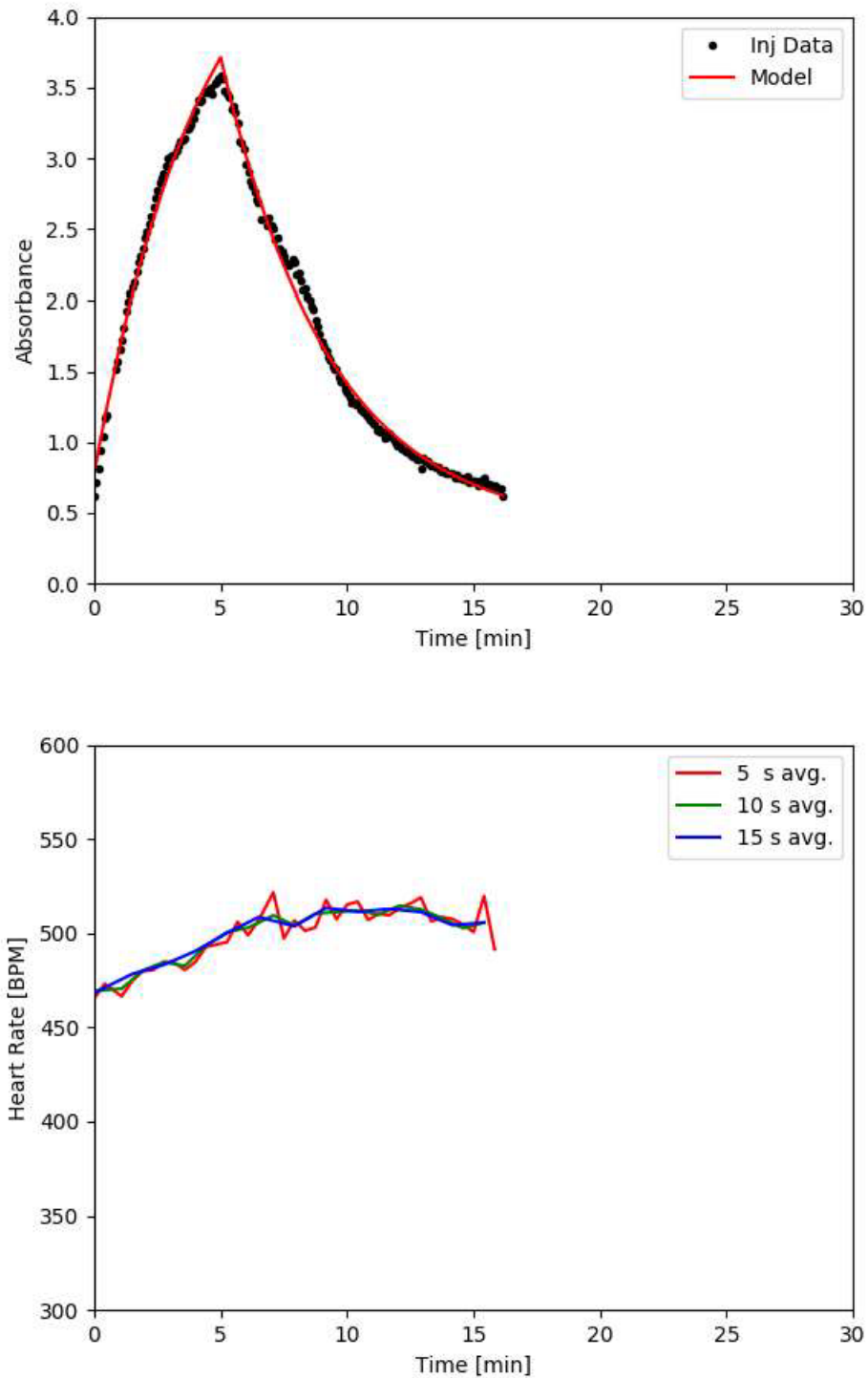


**Figure A-13:** (Top) Injection profile M5I3 (dots) with model (red line) and (bottom) heart rate data averaged over 5 (red line), 10 (green line), and 15 (blue line) seconds.

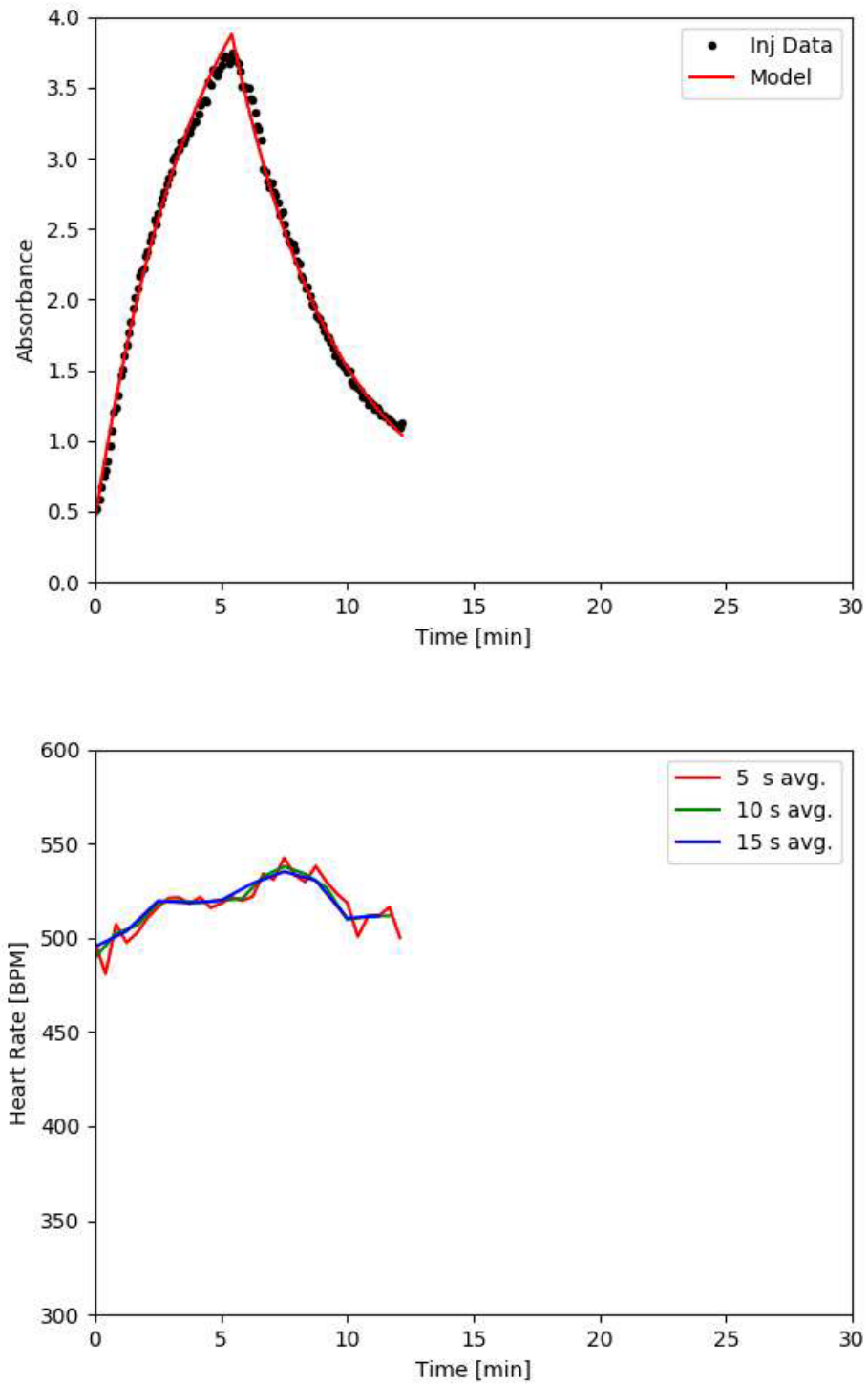


**Figure A-14:** (Top) Injection profile M5I4 (dots) with model (red line) and (bottom) heart rate data averaged over 5 (red line), 10 (green line), and 15 (blue line) seconds.

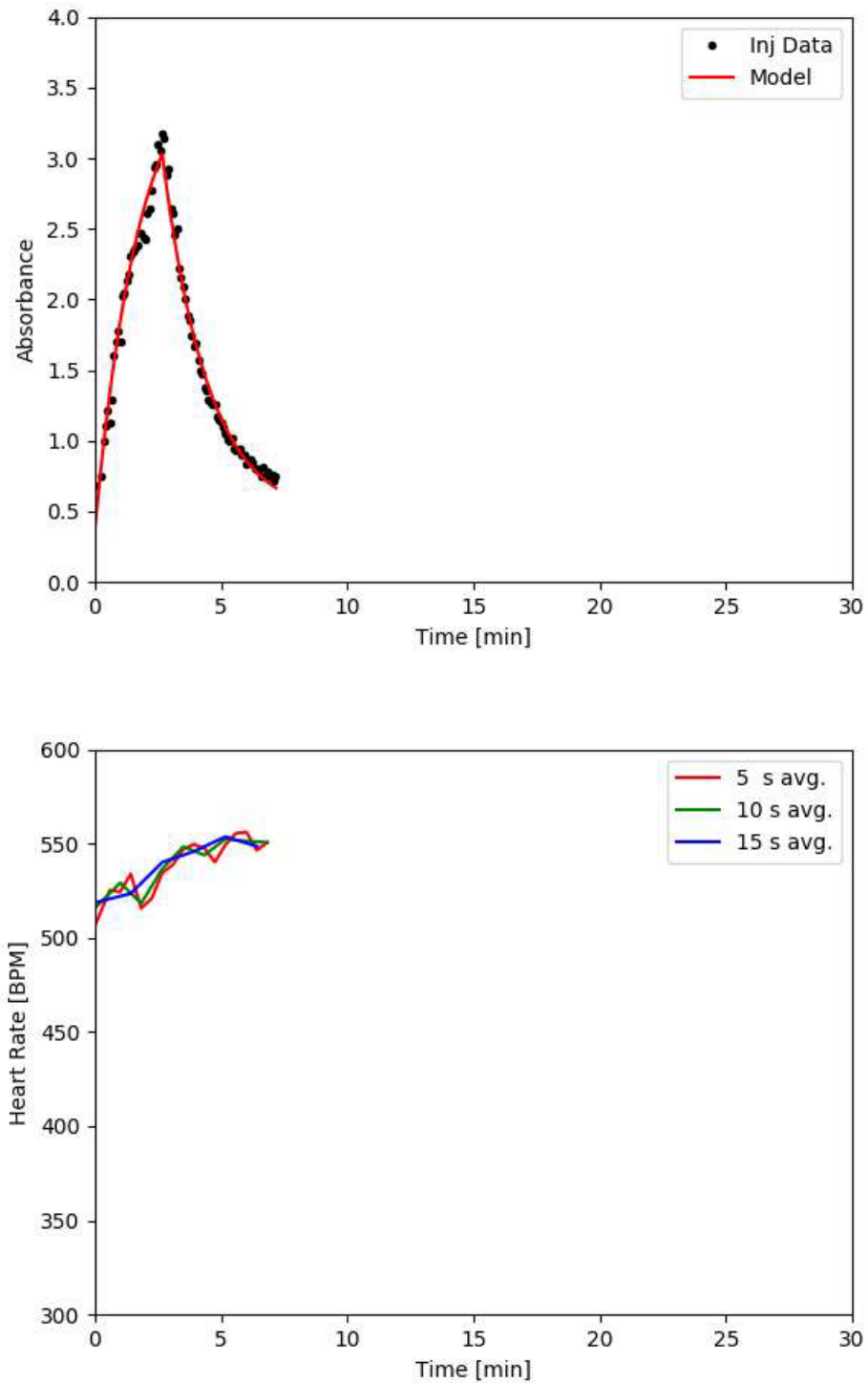


**Figure A-15:** (Top) Injection profile M6I1 (dots) with model (red line) and (bottom) heart rate data averaged over 5 (red line), 10 (green line), and 15 (blue line) seconds.

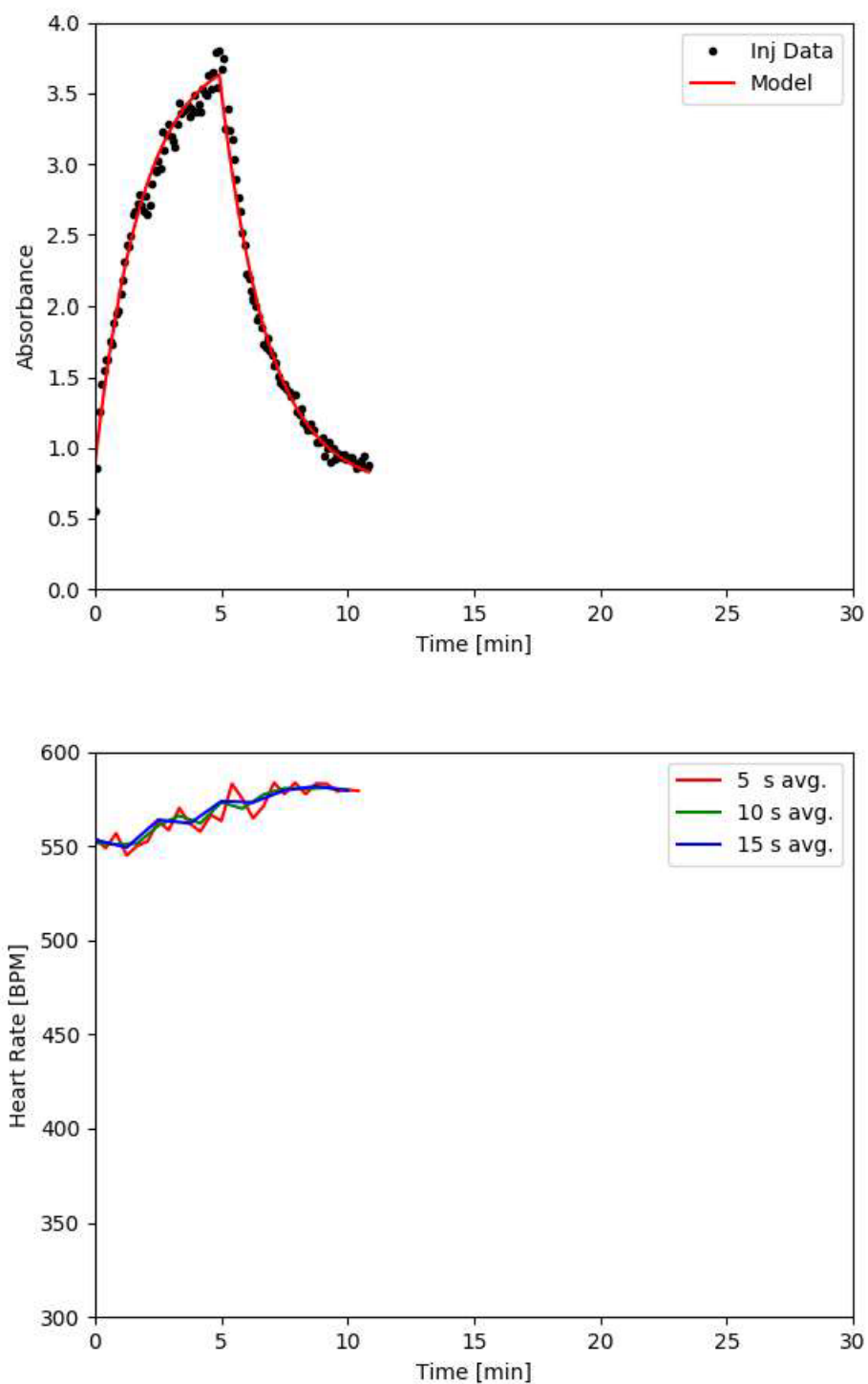


**Figure A-16:** (Top) Injection profile M6I2 (dots) with model (red line) and (bottom) heart rate data averaged over 5 (red line), 10 (green line), and 15 (blue line) seconds.

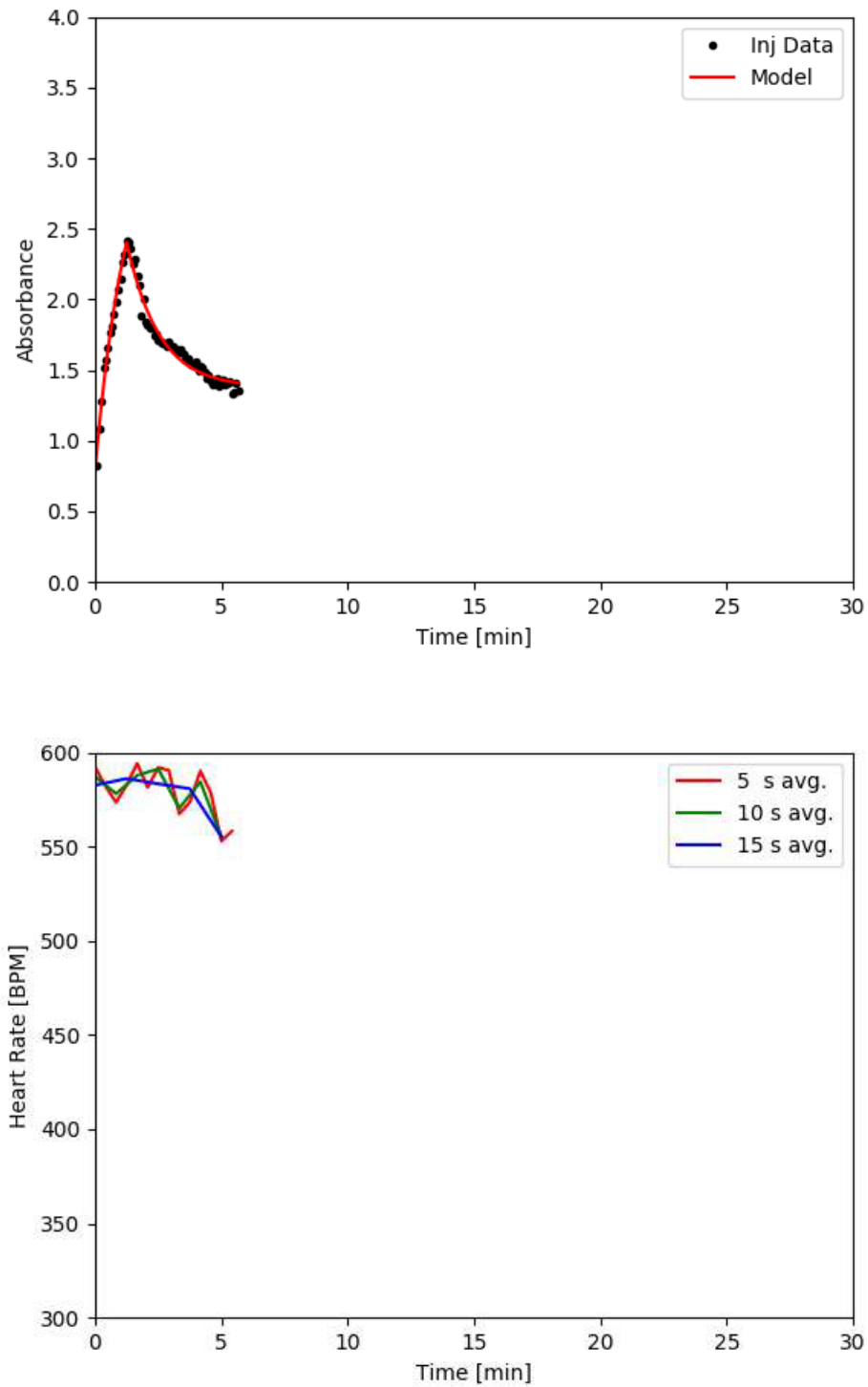


**Figure A-17:** (Top) Injection profile M6I3 (dots) with model (red line) and (bottom) heart rate data averaged over 5 (red line), 10 (green line), and 15 (blue line) seconds.

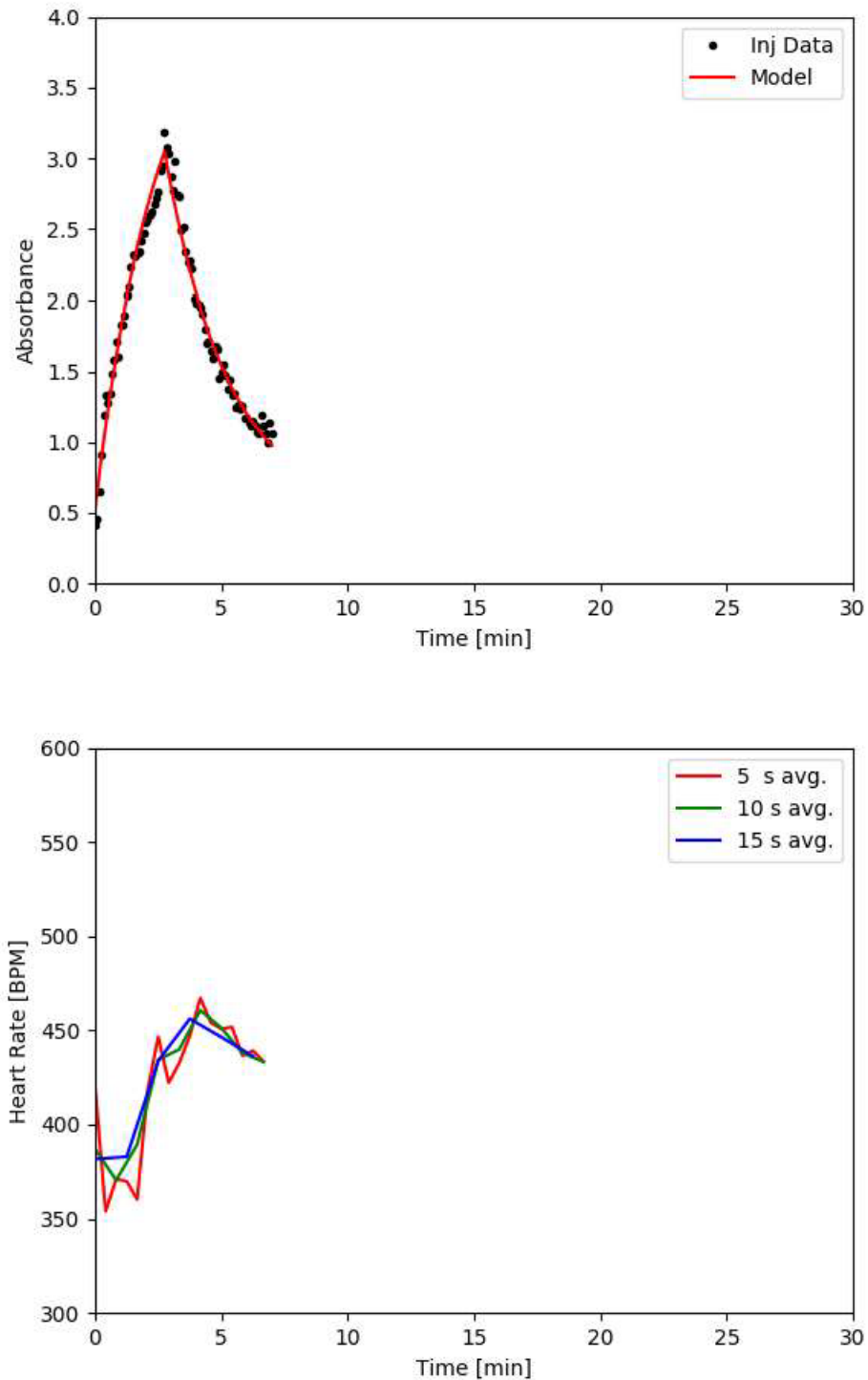


**Figure A-18:** (Top) Injection profile M7I1 (dots) with model (red line) and (bottom) heart rate data averaged over 5 (red line), 10 (green line), and 15 (blue line) seconds.

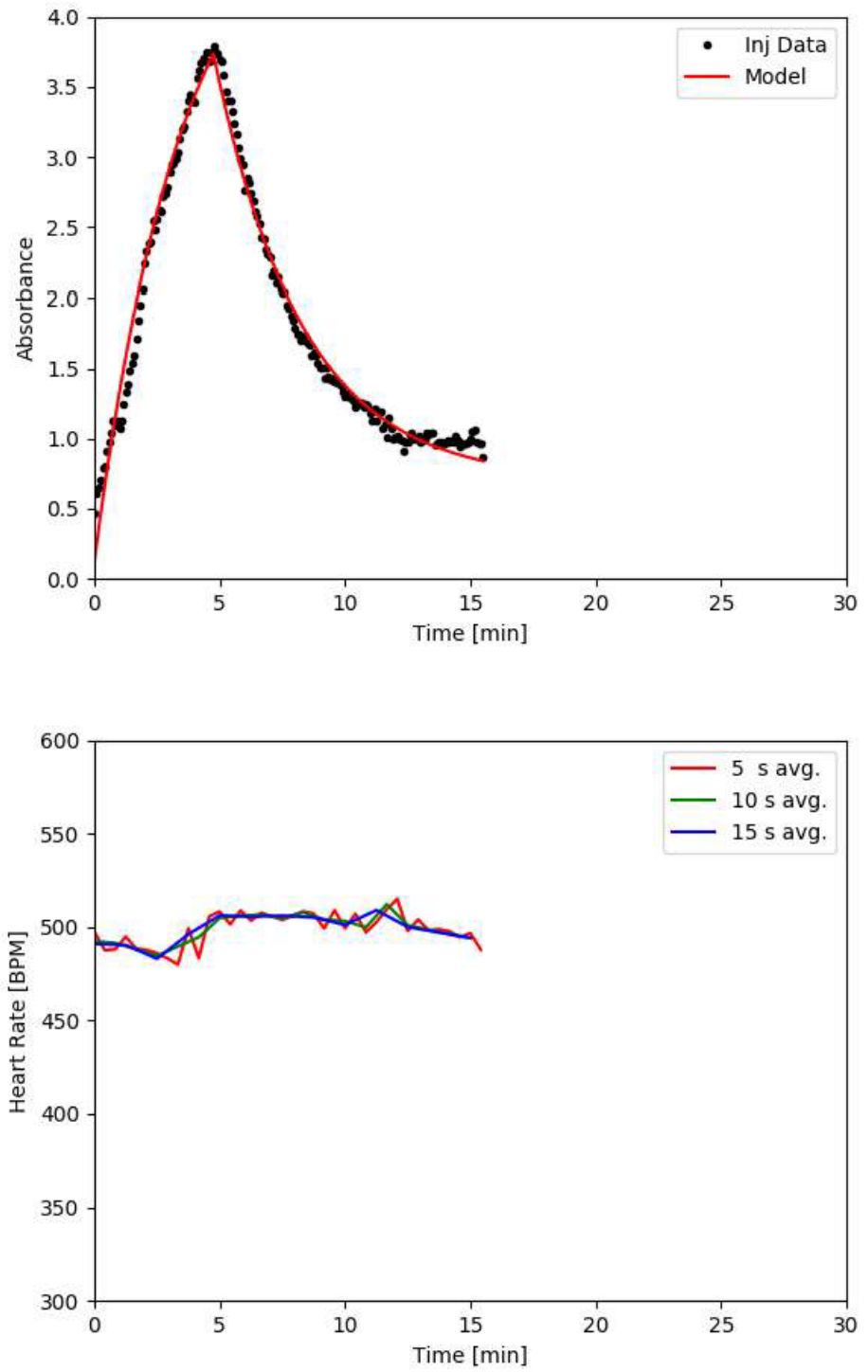


**Figure A-19:** (Top) Injection profile M8I1 (dots) with model (red line) and (bottom) heart rate data averaged over 5 (red line), 10 (green line), and 15 (blue line) seconds.

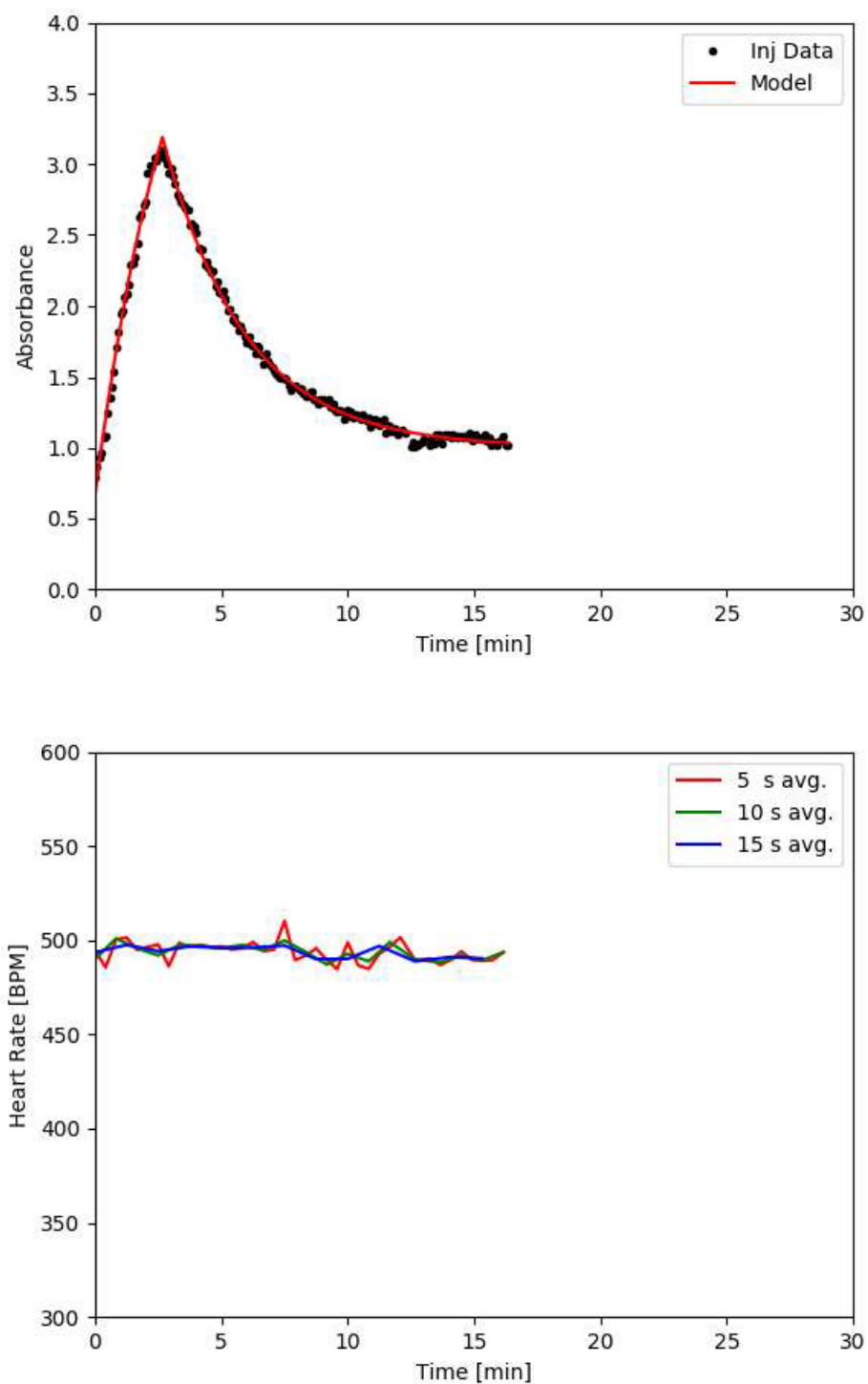


**Figure A-20:** (Top) Injection profile M8I2 (dots) with model (red line) and (bottom) heart rate data averaged over 5 (red line), 10 (green line), and 15 (blue line) seconds.

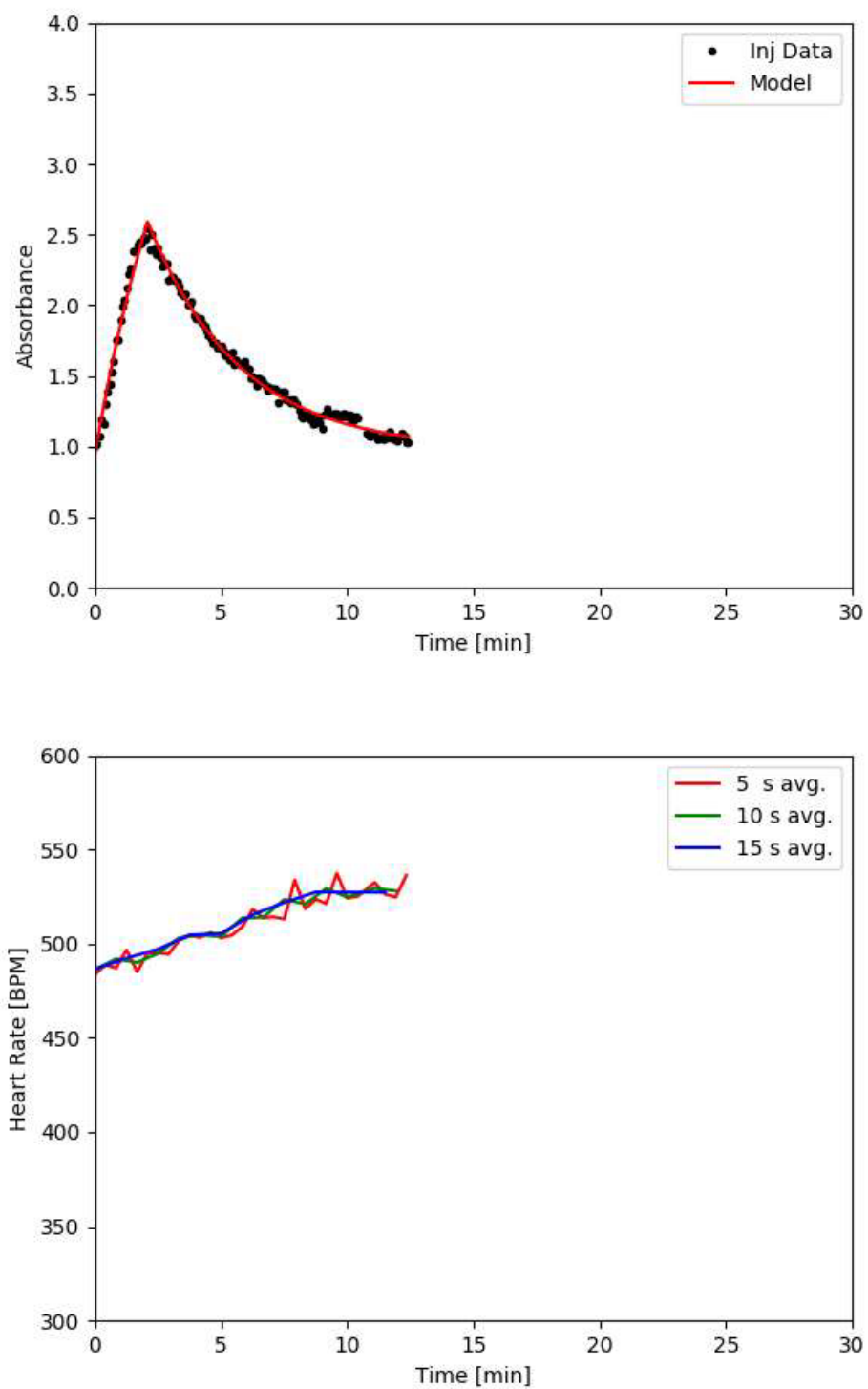


**Figure A-21:** (Top) Injection profile M8I3 (dots) with model (red line) and (bottom) heart rate data averaged over 5 (red line), 10 (green line), and 15 (blue line) seconds.

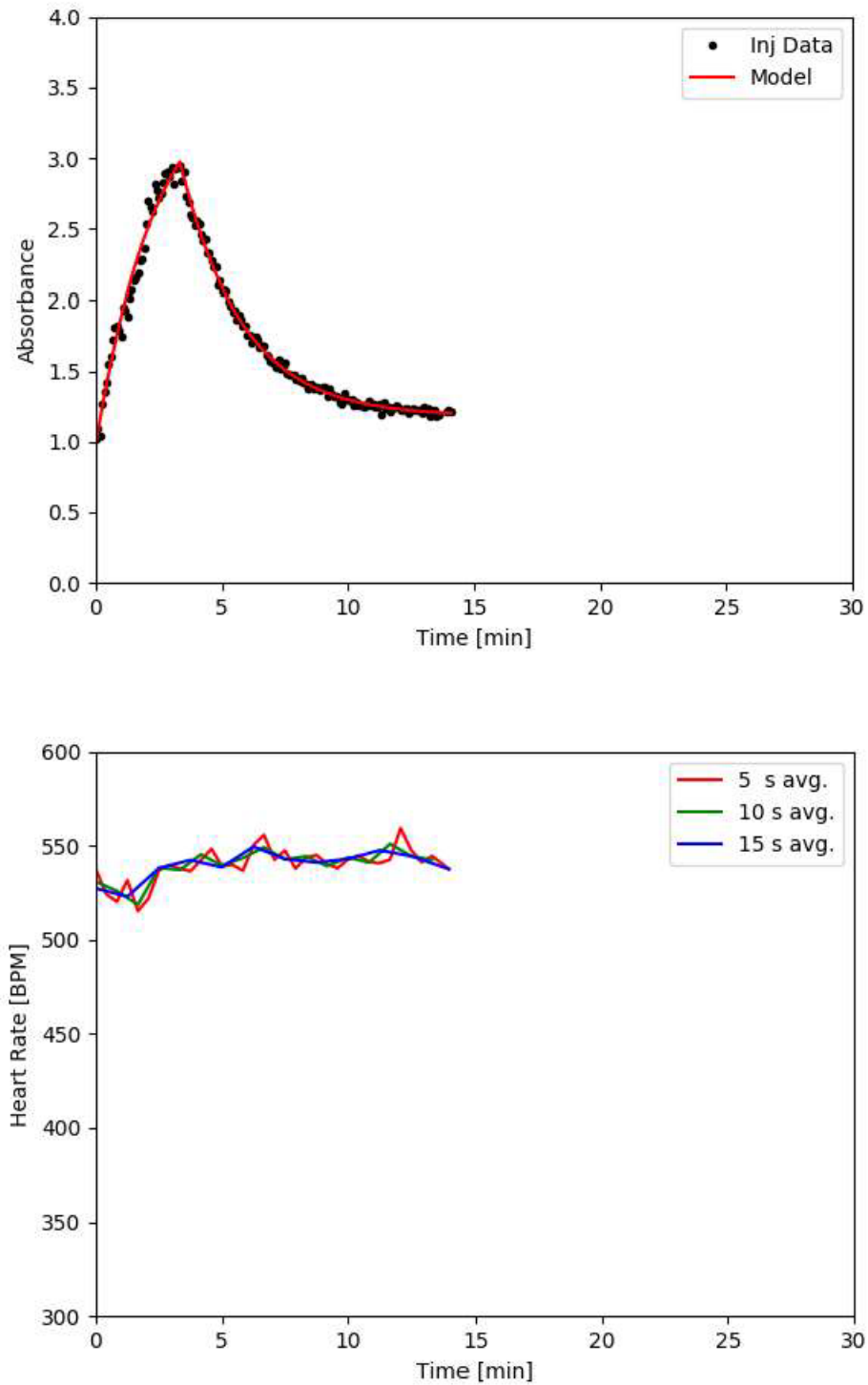


**Figure A-22:** (Top) Injection profile M8I4 (dots) with model (red line) and (bottom) heart rate data averaged over 5 (red line), 10 (green line), and 15 (blue line) seconds.

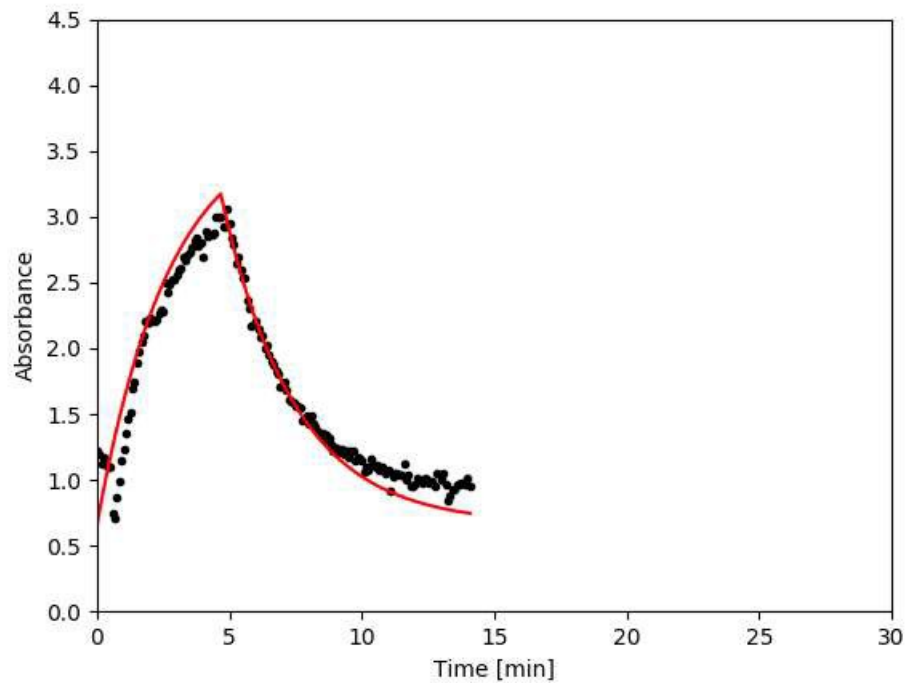


**Figure A-23:** Validation Injection profile M1I1, (dots) with population model (red line).

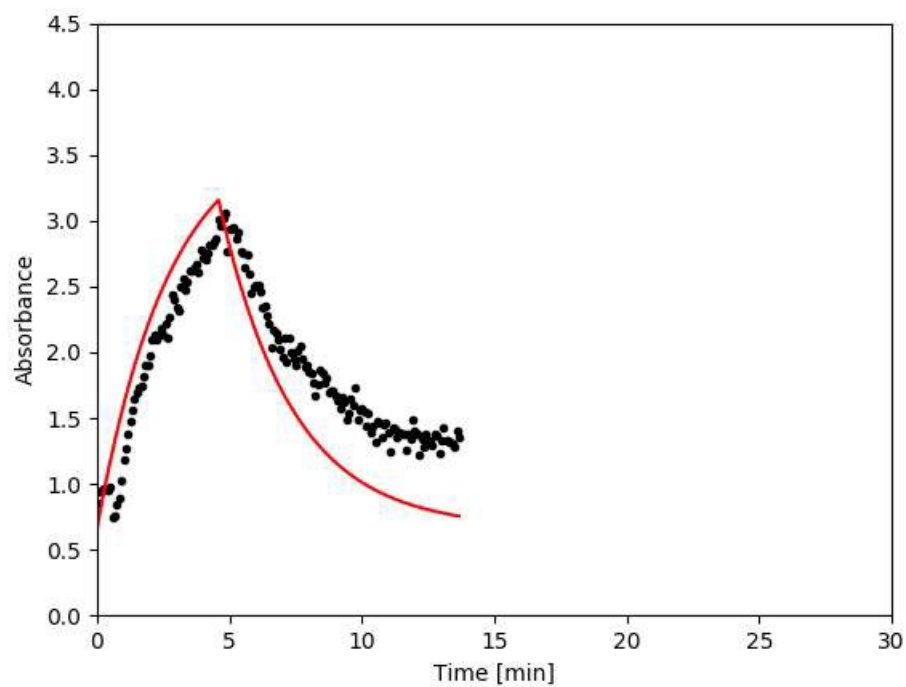


**Figure A-24:** Validation Injection profile M1I2, (dots) with population model (red line).

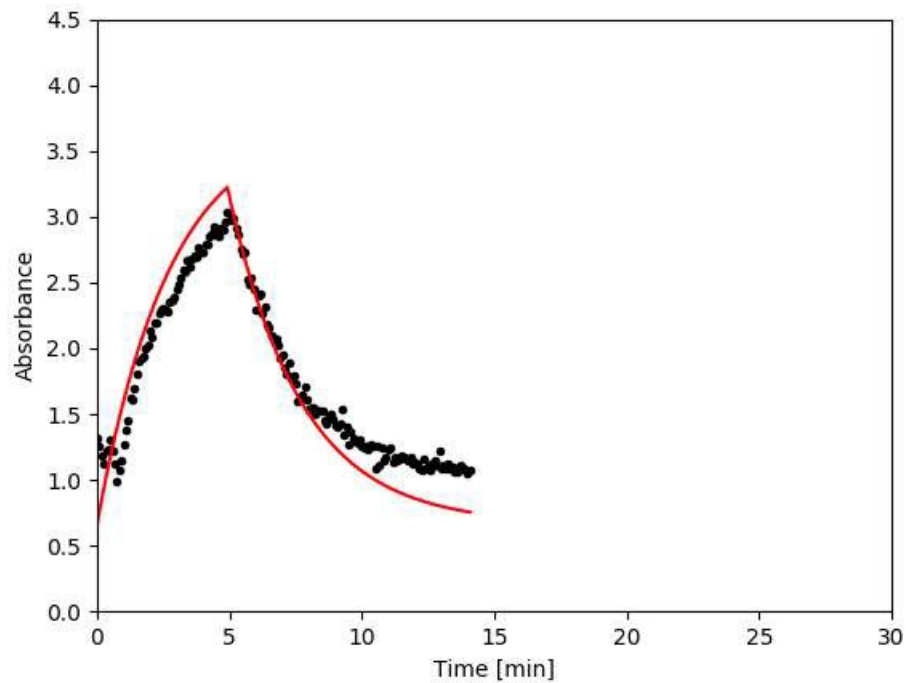


**Figure A-25:** Validation Injection profile M1I3 (dots) with population model (red line).

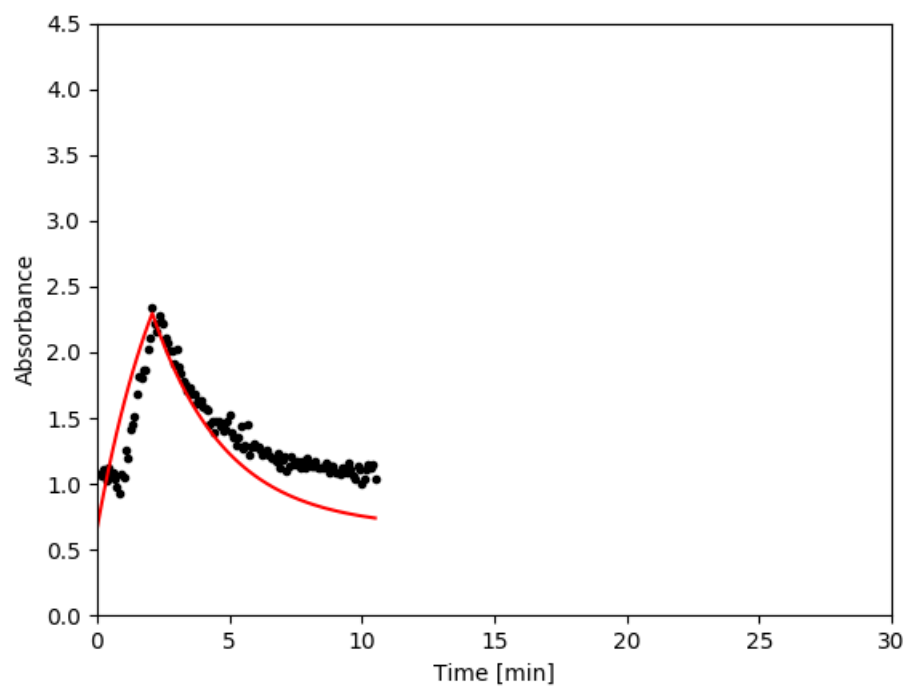


**Figure A-26:** Validation Injection profile M1I4 (dots) with population model (red line).

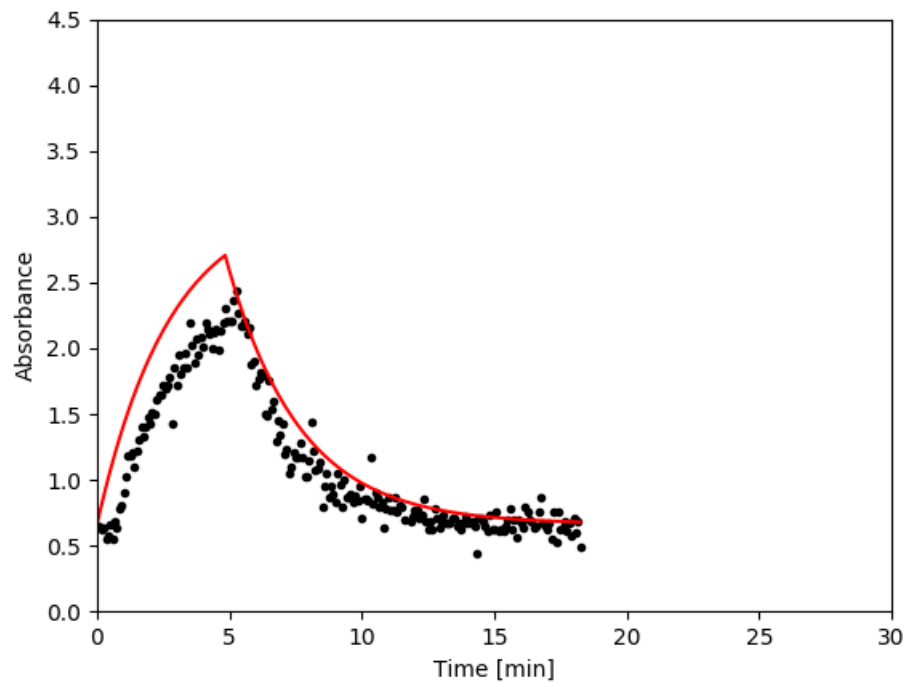


**Figure A-27:** Validation Injection profile M2I1 (dots) with population model (red line).

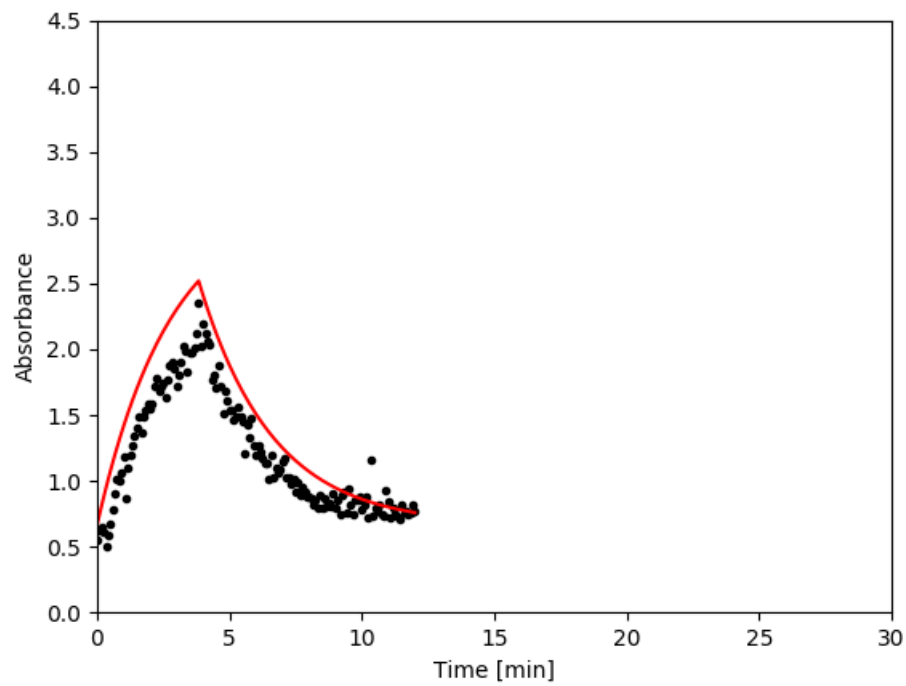


**Figure A-28:** Validation Injection profile M2I2 (dots) with population model (red line).

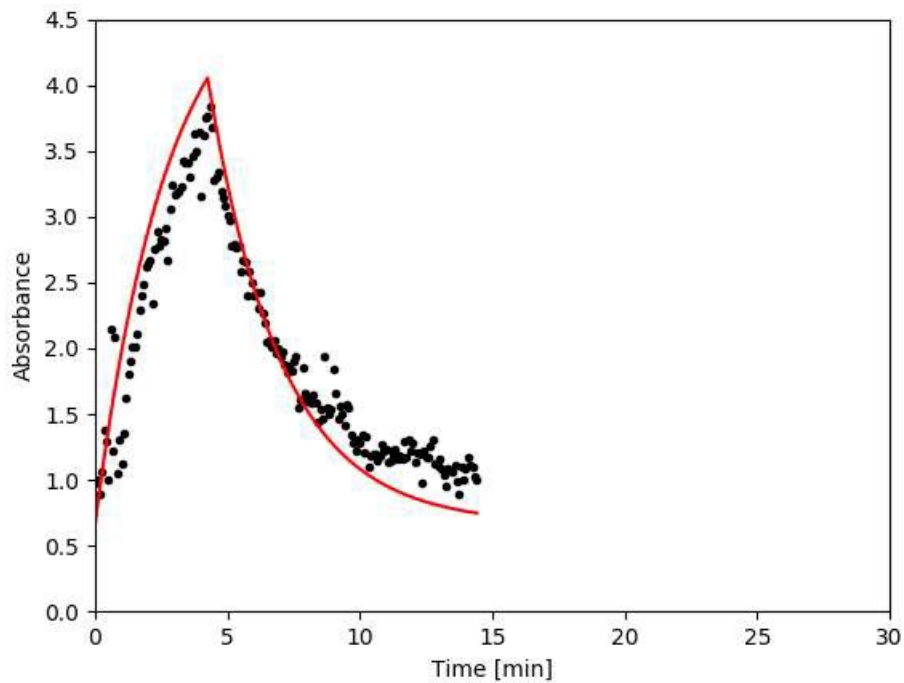


**Figure A-29:** Validation Injection profile M2I3 (dots) with population model (red line).

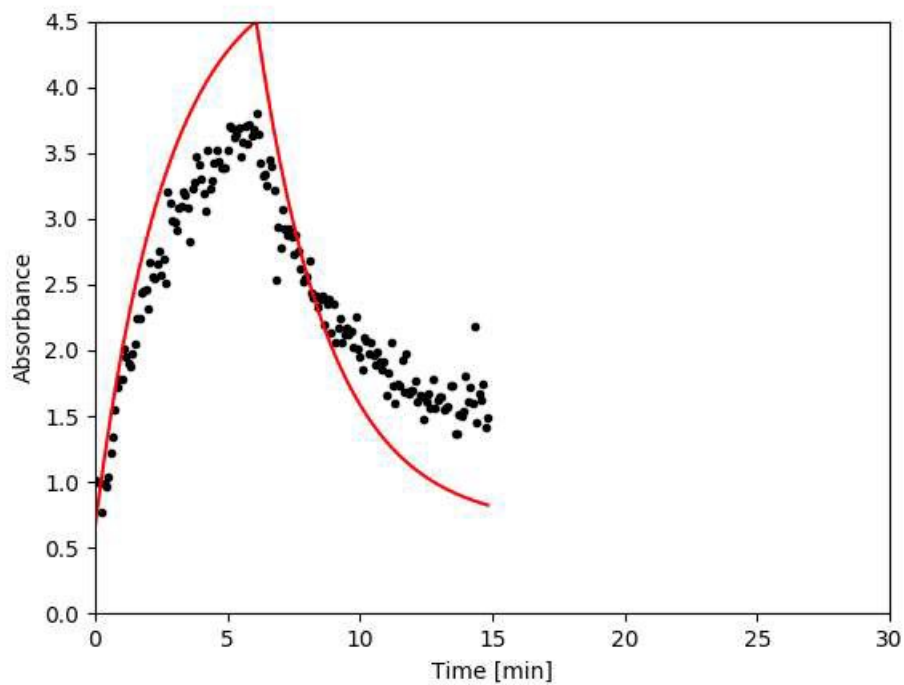


**Figure A-30:** Validation Injection profile M2I4 (dots) with population model (red line).

## **APPENDIX B**

### **CODE FOR SOFTWARE & STATISICAL ANALYSIS**

During the course of this study there were two main programming languages utilized for the development of the software and the statistical analysis of the data. The language selected for the creation of the software was Python v3.3. The external modules utilized in the creation of the software were: math, matplotlib, tkinter, os, serial, and time. A process flow diagram, as well as the core code for the software are included here, in Appendix B.

The language chosen for statistical analysis was WinBUGS v.1.4.3. It utilized the R programming language v.3.1.2 as a container language for processing and ease. The R code which was utilized to by WinBUGS is included here, in Appendix B. The included external R modules were R2WinBUGS, coda, lattice, and MASS.

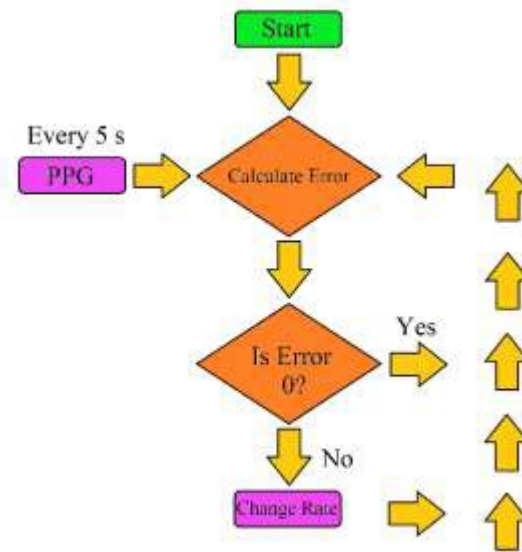


**Figure B-31:** Process flow diagram for Python Control Software.

Below is the core code from the Python program which carried out the process flow described in **Figure B-1**. The red text preceded by a pound-sign are comments, the green text are key words in the python language syntax. The blue text is the name of a defined function. The orange text are text strings. The purple text denotes functions and variables that are properties of the overall class structure. An ellipsis (...) implies the line continues as a truncated line, one line down from the ellipsis.

```

def execute(self):
    # If an Injection has not begun
    if not self.on:
        # Activate Injection
        self.on = 1
        self.stop_on = 0
        self.state = 0

        self.menuactive(0)

        # Check if user wants to clear data
        if self.clearvar.get() == 0:
            if self.restart:
                self.query_clear = M.askyesno(message = 'Would you like to clear all...
injection data?', icon = 'question', title = 'Clear Data?')

                if self.query_clear:
                    self.clear_all_data()

        # If we are restarting an injection, and the users asks, clear all data
        if self.clearvar.get() == 1:

```

```

if self.restart:
    self.clear_all_data()

# Attempt to program the pump, raise error if failure.
try:
    self.program_upload()
    self.program_execute()
    self.pump_running = 1
except SerialException:
    self.wind("Serial Communication Error!")
    self.breaker = 0

# Attempt to grab data from PPG/Initial Run-through before loop
try:
    self.updateData()

# Create a Zero-null time index
self.initial_x = float(self.current_line[9])

# Measure time positively from the Zero-null index
self.x[0] = float(self.current_line[9])-self.initial_x
# Get the OD at the current time index
self.y[0] = float(self.current_line[17])
# Set the PID setpoint to the model value at the current time index
self.PID.setPoint(self.injection_model(self.x[0]))
# Calculate the PID error at the current time index
self.error = self.PID.update(self.y[0])
# Pass the current OD to a past-point container
self.past_od = self.current_line[17]
# Update the Graph
self.update_points()
# Force GUI update in case of any issues.
self.update()

# Numerical Integration to find Injected Volume
self.injected_volume += self.rate_calc_var*0.0666666667
self.injection_var.set(str(round(self.injected_volume, 4))+ ' uL')

# Time-out variable
self.borrow_iterator = time()

# Loop the above (without the definition of a Zero-null index)
while(self.breaker):
    # In the event of any errors, catch them.
    try:
        self.updateData()

        if self.current_line[17] != self.past_od:
            self.x[0] = float(self.current_line[9])-self.initial_x
            self.y[0] = float(self.current_line[17])

            self.PID.setPoint(self.injection_model(self.x[0]))

            self.error = self.PID.update(self.y[0])
            self.PID_err_variable.set(str(round(self.error, 4)))

        if self.state == 0:
            if self.stop_check[0] >= self.stop_val:
                self.stop_command()

        else:
            self.injected_volume += self.rate_calc_var*0.0666666667
            self.injection_var.set(str(round(self.injected_volume, 4))+ ' ul')

```

```

        if abs(self.error) >= self.E_max:
            self.pump_control()

    self.past_od = self.current_line[17]

    self.update_points()

    self.update()

    # Simply ignore any error.
    except IndexError:
        pass

    # Warn the user of a time-out from PPG connection and ask what they'd like
    to do.
    if time()-self.borrow_iterator >= 4:
        if self.pump_running == 1:
            self.query = M.askyesno(message = 'A communication timeout has...
occurred!\n\tStop the Injection?', icon = 'question', title = 'Stop...
Injection?')

            if self.query:
                self.stop_pump()
            else:
                self.wind('A communication timeout has occurred!\nAssumption: Process...
Complete')
                self.menuactive(1)
                self.restart = 1

        break

    # If initial run failed, warn user, only possible case would be a missing file
    from the PPG.
    except FileNotFoundError:
        self.wind('File not Found!')
        self.menuactive(1)

    # Injection is done, tell the system it's not running.
    self.on = 0

    # Ignore successive button presses if we're already running.
    else:
        pass

```

Below is the R utilized for the Bayesian statistical analysis from this project.

```

rm(list = ls())

model_name <- "l_comp_model_analysis"

#####
# set directories and load packages #####
#####

working_directory <- "C:/Users/Trey/Desktop/Research Data/WinBUGS Analysis"
#WinBUGS Analysis"
WinBUGS_directory <- "C:/Users/Trey/Documents/Winbugs"
tools_directory <- "C:/Users/Trey/Documents/Winbugs"

```

```

setwd(working_directory)

library(R2WinBUGS)
library(coda)
library(lattice)
library(MASS)
source(file.path(tools_directory, "bugs.tools.R"))
source(file.path(tools_directory, "bgillespie.utilities.R"))

#####
# data and variables #####
#####

data <- read.csv(file.path(working_directory, "WinBUGS Data.csv"), header=TRUE)

bugsdata <- list(
  N_observations = nrow(data),
  #N_mice = max(data_bolus$MOUSE),
  N_trials = max(data$TRIAL),
  #MOUSE = data$M,
  #GROUP = data_bolus$GROUP,
  TRIAL = data$TRIAL,
  INJ = data$I,
  TIME = data$TIME,
  OD = data$OD, #as.numeric(data$DV),
  TAU = data$TAU,
  CONC = data$CONC,
  HR = data$HRS
  #DOSE = data$DOSE

  #AMT = data_bolus$AMT
  # RATE = data_bolus$RATE
  # DOSE = data_bolus$DOSE,
  # WT = data_bolus$WT
)

bugsinit <- function() {
  rnorm.trunc <- function(n,mean=0,sd=1,lower=-Inf,upper=Inf) {
    qnorm.trunc(runif(n),mean,sd,lower,upper)
  }
  qnorm.trunc <- function(p,mean=0,sd=1,lower=-Inf,upper=Inf) {
    qnorm(p*pnorm(upper,mean,sd)+(1-p)*pnorm(lower,mean,sd),mean,sd)
  }
}

list(
  CL_0 = rnorm.trunc(1, 1.097, 0.1, lower=0),
  CL_precision = rnorm.trunc(1, 6.016, 0.6, lower=0),
  V_0 = rnorm.trunc(1, 3.016, 0.3, lower=0),
  V_precision = rnorm.trunc(1, 1.796, 0.1, lower=0),
  phi_s_0 = rnorm(1, 0.662, 0.06),
  phi_s_precision = rnorm.trunc(1, 17.466, 0.1, lower=0),
  X_precision = rnorm.trunc(1, 1.392, 0.1, lower=0)
  #beta = rnorm(1, 0, 1)
  #beta_l = rnorm(1, 0, 0.001),
  #beta_m = rnorm(1, 0, 0.001),
  #beta_s = rnorm(1, 0, 0.001)

  #beta_group_CL_A = rnorm(1, 0, 0.1),
  #beta_group_CL_B = rnorm(1, 0, 0.1),
  #beta_group_CL_D = rnorm(1, 0, 0.1),
  #beta_injection_CL = rnorm(1, 0, 0.1),
  #beta_group_V_A = rnorm(1, 0, 0.1),
  #beta_group_V_B = rnorm(1, 0, 0.1),

```

```

#beta_group_V_D = rnorm(1, 0, 0.1),
#beta_injection_V = rnorm(1, 0, 0.1),
#beta_preinjection_V = rnorm(1, 0, 0.1),
#beta_preinjection_CL = rnorm(1, 0, 0.1),
#beta_carrageenan_CL = rnorm(1, 0, 0.1)
)
}

parametersToPlot <- c("CL_0", "V_0", "phi_s_0", "X_sigma", "CL_sigma",
"V_sigma", "phi_s_sigma", "CL_trial", "V_trial", "phi_s_trial")
# "beta_preinjection_CL", "beta_group_V_A", "beta_group_V_B",
"beta_group_V_D", "beta_group_CL_A", "beta_group_CL_B", "beta_group_CL_D",
"beta_injection_CL", "CL_mouse", "V_mouse", "CL_sigma_mouse", "V_sigma_mouse"

otherRVs <- c()

parameters <- c(parametersToPlot, otherRVs)
parametersToPlot <- c("deviance", parametersToPlot)

#####
# run WinBUGS #####
#####

#n.chains <- 2
#n.iter <- 2000
#n.burnin <- 1000
#n.thin <- 1

n.chains <- 5
n.iter <- 20000
n.burnin <- 10000
n.thin <- 5

bugs.fit <- bugs(
  data = bugsdata,
  inits = bugsinit,
  parameters.to.save = parameters,
  model.file = file.path(working_directory, paste(model_name, ".txt",
sep="")),
  n.chains = n.chains,
  n.iter = n.iter,
  n.burnin = n.burnin,
  n.thin = n.thin,
  clearWD = FALSE,
  debug = FALSE,
  bugs.directory = WinBUGS_directory,
  working.directory = getwd()
)
WinBUGS_output = bugs.fit$sims.array
posterior = array(as.vector(WinBUGS_output),
dim=c(prod(dim(WinBUGS_output)[1:2]), dim(WinBUGS_output)[3]),
dimnames=list(NULL,dimnames(WinBUGS_output)[[3]]))
posterior <- subset(posterior, select=c(-deviance))
#write.csv(posterior, file="C:/Users/Eric_Sherer/Dropbox/Project -
Omnibus/PK_analysis_average/posterior.csv", row.names=FALSE)

temp =
WinBUGS_output[, ,unlist(sapply(c(paste("^",parametersToPlot,"$",sep=""),paste("
^",parametersToPlot,"\\[",sep="")),grep,x=dimnames(WinBUGS_output)[[3]]))]
summary_table = parameter.plot.table(temp)
write.csv(summary_table, paste("summary.csv",sep=""))

```

## BIBLIOGRAPHY

- [1] S. Edwards, and S. Axe, "The ten 'R's of safe multidisciplinary drug administration", *Nurse Prescribing*, vol. 13, no. 8, pp. 352-360, 2015.
- [2] A. U. Schubert, M. Janda, O. Simanski, J. Bajorat, B. Pohl, R. Hofmockel, and B. Lampe, "A Fuzzy System for Regulation of the Analgesic Remifentanyl during General Anaesthesia", 16th Mediterranean Conference on Control and Automation, 1634-1639, 2008.
- [3] M. Mahfouf, M. Abbod and D. Linkens, "A survey of fuzzy logic monitoring and control utilisation in medicine", *Artificial Intelligence in Medicine*, vol. 21, no. 1-3, pp. 27-42, 2001.
- [4] A. Absalom and G. Kenny, "Closed-loop control of propofol anaesthesia using bispectral index<sup>TM</sup>: performance assessment in patients receiving computer-controlled propofol and manually controlled remifentanyl infusions for minor surgery", *British Journal of Anaesthesia*, vol. 90, no. 6, pp. 737-741, 2003.
- [5] S. Ching, M. Liberman, J. Chemali, M. Westover, J. Kenny, K. Solt, P. Purdon and E. Brown, "Real-time Closed-loop Control in a Rodent Model of Medically Induced Coma Using Burst Suppression", *Anesthesiology*, vol. 119, no. 4, pp. 848-860, 2013.
- [6] A. Fields, K. Fields and J. Cannon, "Closed-loop systems for drug delivery", *Current Opinion in Anaesthesiology*, vol. 21, no. 4, pp. 446-451, 2008.
- [7] M. Shanechi, J. Chemali, M. Liberman, K. Solt and E. Brown, "A Brain-Machine Interface for Control of Medically-Induced Coma", *PLoS Comput Biol*, vol. 9, no. 10, p. e1003284, 2013.
- [8] D. O'Neal, L. Hirsch, N. Halas, J. Payne and J. West, "Photo-thermal tumor ablation in mice using near infrared-absorbing nanoparticles", *Cancer Letters*, vol. 209, no. 2, pp. 171-176, 2004.
- [9] P. Adhikari, W. Eklund, D. O'Neal, "Non-invasive in vivo monitoring of circulating amphotericin b using multi-wavelength photoplethysmography", *Proc. SPIE*, vol. 9332, no. 93320H, 2015.

- [10] P. Adhikari, W. Eklund, E. Sherer, D. O'Neal, "Assessment of multi-wavelength pulse photometry for non-invasive does estimation of circulating drugs and nanoparticles", Proc. SPIE, vol. 9715, no. 9750O, 2016.
- [11] I. Magaña, "Improving Practices in Nanomedicine Through Near Real-Time Pharmacokinetic Analysis", Ph. D, Louisiana Tech University, 2015.
- [12] M. Inoue, F. Kajiya, H. Inada, A. Kitabatake, M.Hori, S. Fukui, H. Abe, "Optimal Control of Meidcal Treatment: Adaptive control of Blood Glucose Level in Diabetic Coma", Computers and Biomedical Research, vol. 9, 217-228, 1976.
- [13] H. Moradi, G. Vossoughi, H. Salarieh, "Optimal robust control of drug delivery in cancer chemotherapy: A Comparison between three control approaches", Computer Methods and Programs in Biomedicine, vol. 112, 69-83, 2013.
- [14] D. Lunn, C. Jackson, N. Best, A. Thomas, and D. Spiegelhalter, "The BUGS Book", CRC Press, 2013.
- [15] M. L. J. Landsman, G. Kwant, G. A. Mook, W. G. Zijlstra, "Light- absorbing properties, stability, and spectral stabilization of indocyanine green," J. Appl. Physiol.,40, 575-583, 1976.
- [16] G. Michalak, J. Schwartz, G. Goodrich and D. O'Neal, "Three-wavelength murine photoplethysmography for estimation of vascular gold nanorod concentration", Opt. Express, vol. 18, no. 25, p. 26535, 2010.
- [17] National Instruments, "PID Theory Explained", <http://www.ni.com/white-paper/3782/en/>, pp. 1-4, March 29, 2011.
- [18] G. Silva, A. Datta, and S. Bhattacharyya, "PID Controllers for Time-Delay Systems", Birkhäuser, 2005.
- [19] T. Desmettre, J. Devoisselle and S. Mordon, "Fluorescence Properties and Metabolic Features of Indocyanine Green (ICG) as Related to Angiography", Survey of Ophthalmology, vol. 45, no. 1, pp. 15-27, 2000.